

On the role of circulation and mixing in the ventilation of OMZs

P. Brandt et al.

On the role of circulation and mixing in the ventilation of oxygen minimum zones with a focus on the eastern tropical North Atlantic

P. Brandt¹, D. Banyte¹, M. Dengler¹, S.-H. Didwischus¹, T. Fischer¹, R. J. Greatbatch¹, J. Hahn¹, T. Kanzow^{1,*}, J. Karstensen¹, A. Körtzinger¹, G. Krahnemann¹, S. Schmidtke¹, L. Stramma¹, T. Tanhua¹, and M. Visbeck¹

¹GEOMAR Helmholtz-Zentrum für Ozeanforschung Kiel, Kiel, Germany

* now at: Alfred-Wegener-Institut Helmholtz-Zentrum für Polar- und Meeresforschung, Bremerhaven, Germany

Received: 17 July 2014 – Accepted: 27 July 2014 – Published: 7 August 2014

Correspondence to: P. Brandt (pbrandt@geomar.de)

Published by Copernicus Publications on behalf of the European Geosciences Union.

Title Page

Abstract

Introduction

Conclusions

References

Tables

Figures



Back

Close

Full Screen / Esc

Printer-friendly Version

Interactive Discussion



1 Introduction

The oceanic oxygen distribution is generally characterized by slightly supersaturated oxygen levels in the surface layer, an intermediate oxygen minimum, and higher oxygen levels at depth. This vertical structure is a consequence of the delicate balance between the supply of oxygen through ventilation and circulation, and oxygen consumption by remineralization of sinking organic matter. The horizontal distribution of oxygen shows major large scale open ocean subsurface oxygen minimum zones (OMZs) in the eastern parts of the tropical Atlantic and Pacific Oceans as well as in the northern Indian Ocean. By analysing a combination of historical and modern observations, an expansion and intensification of OMZs in the tropical oceans has been detected (Stramma et al., 2008b). However, numerical simulations with global or regional models are not able to consistently reproduce such trends and thus up to now fail to provide an explanation of the observed oxygen trends in the tropical ocean (Stramma et al., 2012).

OMZs in the tropical Atlantic were first identified by analysing hydrographic data from the German Meteor Expedition during 1925 to 1927 (Wattenberg, 1938). This dataset revealed the existence of OMZs in both hemispheres of the eastern tropical Atlantic at a depth between 300 and 700 m, situated equatorward of the subtropical gyres and separated by an equatorial oxygen maximum. Based on data, including those from the German Meteor Expedition, as well as theoretical considerations, Wyrki (1962) concluded that the boundaries of these OMZs are set by advection with the lowest oxygen levels occurring in almost stagnant water bodies. A plausible theory of thermocline ventilation was delivered by Luyten et al. (1983b). The basis of their theory is of an ocean forced by subtropical Ekman pumping and otherwise obeying circulation pathways that are governed by potential vorticity conservation. This theory explains the existence of non-ventilated, near-stagnant shadow zones in the eastern tropics. The remaining slow ventilation of such shadow zones, which in steady state is required to balance oxygen consumption, is expected to be the consequence of lateral fluxes of oxygen

BGD

11, 12069–12136, 2014

On the role of circulation and mixing in the ventilation of OMZs

P. Brandt et al.

Title Page

Abstract

Introduction

Conclusions

References

Tables

Figures

⏪

⏩

◀

▶

Back

Close

Full Screen / Esc

Printer-friendly Version

Interactive Discussion



**On the role of
circulation and
mixing in the
ventilation of OMZs**P. Brandt et al.

[Title Page](#)[Abstract](#)[Introduction](#)[Conclusions](#)[References](#)[Tables](#)[Figures](#)[⏪](#)[⏩](#)[◀](#)[▶](#)[Back](#)[Close](#)[Full Screen / Esc](#)[Printer-friendly Version](#)[Interactive Discussion](#)

to analyse their causes. The present paper provides an overview of the current status of the science regarding these topics. The paper is organized as follows: in Sect. 2, data and methods used in this study are described. In Sect. 3, the current system and the OMZ structure in the ETNA are characterized. Results for the quantification of the strength of different ventilation processes, i.e. vertical mixing, lateral mixing, and advection, are presented in Sect. 4. In Sect. 5, the current knowledge on oxygen consumption estimates is presented. The OMZ structure and processes at the continental margin are presented in Sect. 6. Long-term oxygen variability with a special focus on the period of enhanced data coverage is presented in Sect. 7. The results obtained for the ETNA OMZ are then compared to results obtained for the eastern tropical South Pacific (ETSP) in Sect. 8 and finally, in Sect. 9, the results are summarized and discussed.

2 Observational work within the SFB 754

The SFB 754 addresses climate induced ocean deoxygenation, with a focus on tropical OMZ in the Atlantic and Pacific, and its implications for the global marine biogeochemical system. A major focus of the observational work has been on circulation, ventilation physics, and water mass distribution. In the tropical North Atlantic, observations concentrated on the 23° W section with repeat hydrography, microstructure measurements, velocity measurements (Table 1), and moored observations (Table 2). The 23° W section cuts through the ETNA OMZ from south of the Cape Verde archipelago to slightly south of the equator (Fig. 1). Along the 23° W section, moorings with instrumentation to continuously observe temperature, salinity, oxygen and velocity were deployed at different latitudes (8° N, 5° N, 0°) delivering multi-year time series. Additionally, oxygen sensors were installed at 300 m and 500 m depth at selected moorings (23° W, 4° N and 11.5° N) of the Prediction and Research moored Array in the Tropical Atlantic (PIRATA; Bourles et al., 2008) and at a subsurface mooring at 23° W, 2° N (Fig. 1). For the analysis of hydrographic and velocity data acquired along 23° W, we used, in addition to the

On the role of circulation and mixing in the ventilation of OMZs

P. Brandt et al.

Title Page

Abstract

Introduction

Conclusions

References

Tables

Figures

◀

▶

◀

▶

Back

Close

Full Screen / Esc

Printer-friendly Version

Interactive Discussion



measurements given in Table 1, data from other German, US, and French cruises carried out during 1999 to 2011 as listed in Hahn et al. (2014). Besides the 23° W section, we shall present here also data acquired along 18° N at the northern boundary of the ETNA OMZ (Fig. 1). The 18° N section was, in addition to two cruises listed in Table 1, covered several times during 2005 to 2010 by research cruises (RV *Poseidon* cruises 320/1, 347/1, 348/1, 399/2, RV *Meteor* cruise 68/3). Moreover, two tracer release experiments (TREs) were carried out in the ETNA OMZ. During the first TRE, GUTRE (Guinea Upwelling Tracer Release Experiment), in April 2008, 92 kg of the halocarbon tracer trifluoromethyl sulfur pentafluoride (CF₃SF₅) were released at 23° W, 8° N on the potential density surface, $\sigma_\theta = 26.88 \text{ kg m}^{-3}$. The depth of release, of about 300 m, corresponds to the depth of the oxycline above the deep oxygen minimum. During the following 2.5 years, three tracer surveys were carried out to measure the vertical and horizontal spreading of the tracer (Banyte et al., 2012, Table 1). During the second TRE, OSTRE (Oxygen Supply Tracer Release Experiment), in November 2012, 88.5 kg of the same tracer were released at 21° W, 11° N on the potential density surface $\sigma_\theta = 27.03 \text{ kg m}^{-3}$ corresponding to about 500 m depth which is in the core region of the ETNA OMZ.

In the ETSP OMZ a particular focus was on the ~ 86° W section (section located at 85°50' W north of 15° S with a westward shift to 88° W south of 20° S, called ~ 86° W section in the following) with hydrographic and current measurements from 2° N to about 22° S (Fig. 2). Two cruises covered that section (Table 1) repeating measurements taken during the RV *Knorr* cruise in March 1993. Additionally, three cruises were carried out along the continental margin of Peru (Table 1) to investigate the circulation along the continental slope and shelf off Peru as well as the physical processes contributing to the redistribution of oxygen, nutrients and other solutes.

3 Structure of the ETNA OMZ

The subtropical gyre circulation of the Northern Hemisphere is, to first order, determined by the positive wind stress curl associated with mid-latitude westerlies and north-east trade winds. The resulting Ekman pumping drives subduction of oxygen-rich surface water masses in the subtropics. According to theory, equatorward and westward propagation of subducted water masses forms the northern boundary of the shadow zone of the ventilated thermocline (Luyten et al., 1983b). Within the shadow zone, which is characterized by a weak mean circulation, the ETNA OMZ with a core depth at about 400 m is found. Lowest oxygen concentrations at the core depth are found away from the continental margin at about 20° W, 10° N (Fig. 3). North of the ETNA OMZ is the North Equatorial Current (NEC) flowing southwestward along the Cape Verde Frontal Zone. It transports oxygen-rich Central Water (CW) formed by subduction in the subtropics as well as intermediate water masses in the deeper layers having their origin mainly in the Labrador Sea and the Mediterranean outflow. To the south, the ETNA OMZ is bounded by the energetic zonal flows near the equator forming the equatorial oxygen maximum (Brandt et al., 2012). Above the main deep OMZ, at a depth of about 100 m, a shallow OMZ is situated, defined as the secondary oxygen minimum below the surface mixed layer and above 200 m (Fig. 4). It is characterized by generally higher oxygen levels compared to the deep OMZ, while occasionally extremely low oxygen levels are possible, and is most pronounced in the northeastern part of the shadow zone close to the highly productive eastern boundary upwelling region off Mauritania and Senegal (Fischer et al., 2013). The mean 18° N section shows shallow mixed layer depths at the continental margin typical for coastal upwelling regions as well as lower salinities in the CW layer that are a consequence of the northward transport of Southern Hemisphere water along the continental slope within the Poleward Undercurrent (Barton, 1989) and the surface flow associated with the Mauritania Current (Mittelstaedt, 1983) (Fig. 5).

On the role of circulation and mixing in the ventilation of OMZs

P. Brandt et al.

Title Page

Abstract

Introduction

Conclusions

References

Tables

Figures



Back

Close

Full Screen / Esc

Printer-friendly Version

Interactive Discussion



On the role of circulation and mixing in the ventilation of OMZs

P. Brandt et al.

Title Page

Abstract

Introduction

Conclusions

References

Tables

Figures

◀

▶

◀

▶

Back

Close

Full Screen / Esc

Printer-friendly Version

Interactive Discussion



the ETNA is the presence of an open ocean upwelling regime within the cyclonic circulation of the Guinea Dome south of the Cape Verde archipelago. Associated with the presence of the Guinea Dome are changes in the potential vorticity distribution that further limit the flow of newly subducted water masses from the Northern Hemisphere subtropics toward the equator within the STC (Malanotte-Rizzoli et al., 2000).

Along the 23° W section cutting through the ETNA OMZ (defined, beside low oxygen levels, by the high age of the water masses, see e.g. Schneider et al., 2012), the meridional salinity and temperature gradient on density surfaces can be observed defining the transition between low- and high-saline water masses of southern and northern origin, respectively (Fig. 6). Along this section mean eastward and westward flow is typically identified by high and low oxygen levels (Brandt et al., 2010).

Ventilation time scales of the interior ocean can be quantified by analysing transient tracer distributions. Observational work during the SFB 754 included a comprehensive set of CFC-12 and SF₆ measurements in the ETNA (these tracers are measured in parallel to the deliberately released tracer CF₃SF₅). This data set has been explored in detail by Schneider et al. (2012) using the concept of transit time distributions (TTDs) (e.g. Waugh et al., 2004). The mean age in the centre of the OMZ ($\sigma_{\theta} = 27.0 \text{ kg m}^{-3}$) is in the range of 120 to 180 years (Fig. 7). The mean age refers to the average time it takes for a water parcel to reach a certain location in the interior ocean from the time it was last in contact with the surface ocean and hence atmosphere (see Sect. 5 for more discussion on the TTD concept). In contrast to waters in the OMZ centre, water south of about 5° N is significantly better ventilated with mean ages close to 100 years, reflecting the more energetic circulation in the equatorial region. Roughly the same age is found north of about 13° N close to the Cape Verde Islands despite lower oxygen values in the northern compared to the southern region. Below the poorly ventilated OMZ, the even older AAIW ($\sigma_{\theta} = 27.3 \text{ kg m}^{-3}$) with ventilation times in excess of 500 years is found (close to the detection limit of the CFCs, and thus difficult to accurately quantify), although this water mass has high oxygen concentration. Again, at this density layer

4.1 Vertical mixing

Vertical mixing acts on the vertical oxygen gradients and leads to an oxygen supply to the OMZ via down-gradient oxygen fluxes. In order to estimate the vertical or diapycnal oxygen supply, the diapycnal diffusivity K_ρ as a measure for diapycnal mixing is required. From the diapycnal spread of the deliberately released tracer during GUTRE, a mean diapycnal diffusivity of $(1.2 \pm 0.2) \times 10^{-5} \text{ m}^2 \text{ s}^{-1}$ was derived (Banyte et al., 2012). The tracer was injected on the isopycnal $\sigma_\theta = 26.88 \text{ kg m}^{-3}$ (about 300 m), corresponding to the oxycline above the deep OMZ. GUTRE was accompanied by extensive microstructure and finescale shear measurements that delivered an estimate of $(1.0 \pm 0.2) \times 10^{-5} \text{ m}^2 \text{ s}^{-1}$ for K_ρ for the depth range between 150 and 500 m (Fischer et al., 2013). The value inferred from microstructure measurements only considers diapycnal mixing due to small scale turbulence (Fischer et al., 2013). However, double diffusive enhancement was found to be small ($\sim 0.1 \times 10^{-5} \text{ m}^2 \text{ s}^{-1}$) in this depth interval (Fischer et al., 2013), so the total diffusivities estimated by the two independent methods agree within the error bars. This estimate of diapycnal mixing is considerably larger than the expected background mixing at this latitude (e.g. Gregg et al., 2003), probably due to the presence of rough topography (e.g. the Sierra Leone Rise) in the southern part of the OMZ. Combining K_ρ with simultaneous profiles of the vertical oxygen gradient allows determination of the profile of the diapycnal oxygen flux. Its divergence represents the oxygen supply to the OMZ and amounted to about $1 \mu\text{mol kg}^{-1} \text{ yr}^{-1}$ in the OMZ core, with the required oxygen transported downwards from the upper CW (Fischer et al., 2013).

Deeper ranging microstructure profiles acquired recently allowed us to extend the analysis into the deeper water column down to 800 m depth; i.e. allowed us to estimate the diapycnal oxygen flux from the AAIW below as well. 20 deep microstructure profiles were about equally partitioned to three subregions of the OMZ: a seamount subregion (7% of OMZ area), an abyssal plain subregion (80% of OMZ area), and a transition subregion (13% of OMZ area). They served to estimate the relative shape

BGD

11, 12069–12136, 2014

On the role of circulation and mixing in the ventilation of OMZs

P. Brandt et al.

Title Page

Abstract

Introduction

Conclusions

References

Tables

Figures

◀

▶

◀

▶

Back

Close

Full Screen / Esc

Printer-friendly Version

Interactive Discussion



On the role of circulation and mixing in the ventilation of OMZs

P. Brandt et al.

Title Page

Abstract

Introduction

Conclusions

References

Tables

Figures

◀

▶

◀

▶

Back

Close

Full Screen / Esc

Printer-friendly Version

Interactive Discussion



turbulence on a β -plane (Eden, 2007). The estimates from Banyte et al. (2013) and Hahn et al. (2014) are in good agreement (Fig. 14). The average profile of K_e shows maximum eddy diffusivity close to the surface and decreasing values with depth. Together with the mean oxygen distribution, the estimate of K_e was applied to derive the eddy-driven meridional oxygen flux along 23° W.

As a second method the eddy correlation was used to directly calculate the eddy-driven meridional oxygen flux along isopycnal surfaces using mooring time series of oxygen and velocity acquired at 5° N, 23° W and 8° N, 23° W in the years 2009–2012 and 2011–2012, respectively (see Hahn et al. (2014) for details). Although both estimation methods are accompanied by large uncertainties, a comparison of the results at the mooring sites reveals coherent profiles of the meridional oxygen flux (100–800 m). At the depth of the OMZ they yield a northward oxygen flux towards the centre of the OMZ.

The oxygen that is meridionally supplied to the ETNA OMZ regime by lateral mixing can be derived as the divergence of the eddy-driven meridional oxygen flux. The average profile of the eddy-driven meridional oxygen supply (6 – 14° N, 23° W) derived from the diffusive flux parameterization shows a substantial gain of oxygen at the depth of the OMZ and a loss of oxygen above (Fig. 14).

The tropical and subtropical oceans are generally assumed to be associated with an anisotropic horizontal eddy diffusivity (Banyte et al., 2013; Eden, 2007; Eden and Greatbatch, 2009; Kamenkovich et al., 2009) with larger horizontal eddy diffusivities in the zonal than in the meridional direction. Nevertheless, at the depth of the OMZ core, we consider the zonal eddy flux divergence small compared to the meridional eddy flux divergence, since the 2nd derivative of oxygen is an order of magnitude smaller in the zonal than the meridional direction.

4.3 Advection

We now turn to the remaining ventilation term in the budget; that is, the term associated with zonal advection (meridional advection is assumed to be negligible). We are only

On the role of circulation and mixing in the ventilation of OMZs

P. Brandt et al.

Title Page

Abstract

Introduction

Conclusions

References

Tables

Figures

◀

▶

◀

▶

Back

Close

Full Screen / Esc

Printer-friendly Version

Interactive Discussion



variability (see Fig. 15) on monthly time scales but are almost always unidirectional (especially in the Northern Hemisphere); their longitudinal dependence along the equator is currently uncertain. The EDJ are also thought to be generated by downward propagating Yanai waves, in this case by barotropic instability of these waves as discussed by Hua et al. (2008) (see also d'Orgeville et al., 2007 and Ménesguen et al., 2009). The EDJ show downward phase propagation but upward energy propagation, consistent with the above theory, and lead to variability with a roughly 4.5 year period throughout the water column within 2° latitude on either side of the equator and above about 3000 m depth (Brandt et al., 2011). As shown by Brandt et al. (2012), there is evidence of a corresponding 4.5 year variability in oxygen levels in the same region (Fig. 8, equator) with variability at 300 m depth at 23° W on the equator having a range comparable to the range of the mean oxygen level along the equator across the whole Atlantic.

5 Consumption

Oxygen consumption is a key mechanism for the formation of OMZs (Sverdrup, 1938; Wyrтки, 1962) and, although being a prominent part of the local oxygen budget of the OMZs, it is among the poorest constrained ones. We will consider here only the net consumption that is the combined effect of removal and production of oxygen. Removal of oxygen is related to the metabolism of marine life as well as to elementary chemical reactions, whereas production of oxygen is related to photosynthesis and as such confined to the euphotic zone (e.g. Martz et al., 2008). We will focus in this section on pelagic oxygen consumption; removal of oxygen from the water column by uptake at the sediment–water interface will be discussed in Sect. 6.

Direct observations of oxygen in-situ respiration are rare, primarily due to technical difficulties (e.g. Holtappels et al., 2014). The most commonly applied approach to quantify time and space integrated oxygen removal and production processes is through an *apparent oxygen utilization rate* (AOUR; e.g. Riley, 1951; Jenkins, 1982, 1998; Karstensen et al., 2008; Martz et al., 2008; Stanley et al., 2012). The AOUR

sient tracers). The TTD concept acknowledges the shortcomings in age calculations, which assign a single tracer age to a water parcel, and provides a framework to more realistically characterize the ventilation age (e.g. Waugh et al., 2004) by providing a mean age of the TTD. In a study using a transient tracer data set (up to 2009), Schneider et al. (2012) showed for the ETNA that the TTD obeys an inverse Gaussian function with the two moments Γ and Δ being equal ($\Delta/\Gamma = 1$), where Γ is the mean age and Δ defines the width of the TTD. In the limit of $\Delta/\Gamma = 0$, the mean age of the TTD equals the single tracer age.

Here an extended set of CFC-12, SF₆ and oxygen data collected in the ETNA OMZ is used to apply the TTD approach for exploring the oxygen consumption rate. Using CFC-12 and SF₆ data (SF₆ preferentially used if available and CFC-12 if CFC-12 > 450 ppt, i.e. corresponding to atmospheric mixing ratios at about the end of the near-linear atmospheric increase) the AOOR is calculated using two different Δ/Γ ratios (Fig. 16). Note that the AOOR for $\Delta/\Gamma = 0$ is larger than values reported previously (Fig. 16) that were obtained by using a single tracer age concept applied to data collected in the ventilated gyre (e.g. Karstensen et al., 2008).

The two estimates for $\Delta/\Gamma = 0$ and $\Delta/\Gamma = 1$ represent an upper and lower limit of the AOOR within the ETNA OMZ, respectively. A shortcoming of the TTD concept in this region is its one-dimensionality (single water mass), i.e. it only considers the along-isopycnal mixing of parcels of a single source water mass, which might have encountered different advection and diffusion pathways and thus differ in age and AOU. The influence of diapycnal mixing (Fischer et al., 2013) and the mixing of two or more source waters (e.g. North and South Atlantic Central Water) (Kirchner et al., 2009; Brandt et al., 2010) is not considered by TTD concept, which probably leads to a bias of the resulting AOOR. In fact our AOOR values for $\Delta/\Gamma = 1$ are lower than those calculated by Stanley et al. (2012) for the ventilated gyre region of the western North Atlantic close to Bermuda, where they used the TTD approach with $\Delta/\Gamma = 1$ on tritium (³H) and ³He measurements. They derived AOOR values close to 5 $\mu\text{mol kg}^{-1} \text{yr}^{-1}$ for the potential density level of 27.0 kg m^{-3} that were similar to AOOR values obtained

On the role of circulation and mixing in the ventilation of OMZs

P. Brandt et al.

Title Page

Abstract

Introduction

Conclusions

References

Tables

Figures

◀

▶

◀

▶

Back

Close

Full Screen / Esc

Printer-friendly Version

Interactive Discussion



a minimum at about 20° N (Fig. 4). For the deep OMZ, minimum oxygen levels at the continental margin are found south of 16° N (Machin and Pelegri, 2009).

6.1 Upwelling and circulation

The continental margin of Mauritania and Senegal is part of the Canary eastern boundary upwelling system that extends from the northern tip of the Iberia peninsula at 43° N to south of Dakar at about 10° N (e.g. Mittelstaedt, 1991). Due to changes in wind forcing associated with the migration of the Intertropical Convergence Zone, coastal upwelling off Mauritania and Senegal exhibits a pronounced seasonality. Here winds favorable to upwelling prevail primarily from December to April. The seasonality in upwelling and associated primary production must be reflected in oxygen consumption and thus in water-column oxygen concentrations at the continental margin.

The ventilation of the waters above the continental margin occurs primarily through the Mauritania Current in the surface layer and the Poleward Undercurrent below. Both flows transport relatively oxygen-rich South Atlantic Central Water, which is carried eastward within the NECC and NEUC (Figs. 1 and 6), northward into the upwelling region. Often, these two flows are not distinct from each other (e.g. Pena-Izquierdo et al., 2012). Usually, the Poleward Undercurrent is found attached to the continental slope between 50 and 300 m depth, but it may extend as deep as 1000 m (Mittelstaedt, 1983; Barton, 1989; Hagen, 2001; Pena-Izquierdo et al., 2012). Average along-shore velocities from 18° N (Fig. 5) show dominantly poleward flow in the upper 300 m at the continental slope of Mauritania exceeding 0.05 m s⁻¹ that can be associated with the Mauritania Current and the Poleward Undercurrent. However, the effect of the eddy field and other variability on the mean flow is clearly not averaged out due to the small number of available ship sections.

Previous studies showed that the Mauritania Current exhibits a seasonal behavior (Mittelstaedt, 1991), which was found to be associated with the seasonality of the NECC, suggesting that the ventilation of the water masses above the continental margin also varies seasonally. In boreal winter and early boreal spring, when the NECC

On the role of circulation and mixing in the ventilation of OMZs

P. Brandt et al.

Title Page

Abstract

Introduction

Conclusions

References

Tables

Figures



Back

Close

Full Screen / Esc

Printer-friendly Version

Interactive Discussion



is weak, the Mauritania Current only reaches latitudes of about 14° N, while in boreal summer and early boreal autumn, due to the strengthening of the NECC and the relaxation of the northeast trade winds, the Mauritania Current reaches latitudes of about 20° N (Mittelstaedt, 1991; Stramma et al., 2008a).

Several studies have indicated that most of the water carried northward at the continental margin of Mauritania recirculates in the region off Cape Blanc at about 21° N within a cyclonic gyre (Mittelstaedt, 1983; Pena-Izquierdo et al., 2012). This circulation pattern is in agreement with the regional distribution of oxygen levels within the shallow oxygen minimum that exhibits lowest oxygen concentrations at the continental margin and offshore just south of Cape Blanc (Pena-Izquierdo et al., 2012).

6.2 Benthic oxygen uptake

Oxygen uptake within the benthic region (i.e., the sediment and the immediately overlying water) is largely controlled by sediment oxygen consumption and can be a significant sink for oxygen from the water column above. In contrast to the difficulties of direct measurement of pelagic oxygen consumption, local measurements of sediment oxygen uptake are relatively straightforward to perform with a variety of techniques. Recent developments in measurement techniques include the use of benthic chambers, eddy-correlation techniques, multi-sensor microprofilers and benthic observatories (e.g. Glud, 2008). Total benthic oxygen uptake (TOU), which characterizes all processes consuming oxygen within the benthic region, is commonly measured by enclosure techniques such as benthic chambers. With these systems, the initial oxygen decrease of an overlying well-mixed water phase is approximately linear. TOU is then calculated based on the rate of oxygen decrease, accounting for the enclosed area and water volume. TOU rates have recently been measured in the upper 1000 m on the continental slope and shelf off Mauritania using benthic chambers attached to landers (Dale et al., 2014). The reported TOU rates that are quantified in terms of oxygen fluxes into the sediments were as high as $10 \text{ mmol m}^{-2} \text{ d}^{-1}$ in depths between 50 and 100 m and decreased quasi-exponentially to about $3 \text{ mmol m}^{-2} \text{ d}^{-1}$ in a depth of

On the role of circulation and mixing in the ventilation of OMZs

P. Brandt et al.

Title Page

Abstract

Introduction

Conclusions

References

Tables

Figures

◀

▶

◀

▶

Back

Close

Full Screen / Esc

Printer-friendly Version

Interactive Discussion



1000 m. To compare TOU rates to pelagic oxygen consumption, we have to apply the TOU to a water volume with a given in-situ density: the consumption within a 1 m thick layer above the bottom due to TOU is three orders of magnitudes larger when compared to pelagic oxygen consumption occurring at similar depths. This is due to the volume-specific production and degradation of organic material in surface sediments, which supports high densities of microbes and metazoans (Glud, 2008). In shelf areas, it is estimated that 10 to 50 % of the pelagic primary production reaches the sediment (Canfield, 1993; Wollast, 1998) and benthic remineralization plays a key role in this region for the recycling of nutrients and burial of carbon.

Although the benthic oxygen consumption due to TOU at the shelf strongly exceeds pelagic oxygen consumption, benthic processes play a minor role for oxygen depletion within larger volumes as the deep OMZ. To illustrate this, we assume that oxygen depleted water masses are laterally exchanged between the shelf and the open ocean. Between 300 and 600 m depth the continental margin has a typical average topographic slope of about 4 % corresponding to 25 m shelf width per 1 m depth change. Assuming a TOU of $5 \text{ mmol m}^{-2} \text{ d}^{-1}$ results in an oxygen depletion by the sediments of 125 mmol d^{-1} per 1 m depth range and 1 m along-shelf distance. Using the range of pelagic oxygen consumption determined in Sect. 5 (1 to $5 \text{ } \mu\text{mol kg}^{-1} \text{ yr}^{-1}$) and corresponding in-situ density, the equivalent water volume consuming 125 mmol d^{-1} would be $44 \times 10^3 \text{ m}^3$ to $9 \times 10^3 \text{ m}^3$, corresponding to a distance from the shelf, where both processes have comparable influence, of 44 km to 9 km. In other words, pelagic oxygen consumption within the deep OMZ, typically extending about 1000 km offshore, is 1 to 2 orders of magnitude larger than benthic oxygen consumption due to oxygen fluxes into the continental slope sediments. Reduced topographic slopes at shallower depths suggest a more important role of benthic oxygen uptake for the shallow OMZ, which is characterized by minimum oxygen concentration close to the continental margin and is not as widespread as its deeper counterpart (cf. Figs. 3 and 4).

On the role of circulation and mixing in the ventilation of OMZs

P. Brandt et al.

[Title Page](#)[Abstract](#)[Introduction](#)[Conclusions](#)[References](#)[Tables](#)[Figures](#)[Back](#)[Close](#)[Full Screen / Esc](#)[Printer-friendly Version](#)[Interactive Discussion](#)

6.3 Diapycnal oxygen fluxes at the continental margin

Diapycnal mixing on continental slopes and shelf is often found to be elevated due to tides interacting with topographic boundaries that accelerate an energy cascade from large scale open ocean tides to small scale turbulence (e.g. Sandstrom and Oakey, 1995). As shown by Schafstall et al. (2010), diapycnal mixing along the upper continental slope and lower shelf region of the Mauritanian upwelling is strongly elevated due to the presence of nonlinear internal waves that are boosted by the interaction of the barotropic tide with critically sloping topography (e.g. Holloway, 1985). Diapycnal nutrient fluxes calculated for the upwelling region are amongst the highest reported to date (Schafstall et al., 2010).

To assess the role of diapycnal mixing for ventilating the upper layer of the ocean above the continental slope, the diapycnal oxygen flux was calculated from microstructure profiles along with CTD-O₂ profiles collected during two boreal winter cruises on the shelf of Mauritania (for details of the data set used see Schafstall et al., 2010). Mixing on the continental slope and shelf off Mauritania is elevated in the region with a water depth shallower than 500 m (Schafstall et al., 2010). Within this region, the diapycnal flux of oxygen from the mixed layer into the stratified ocean is above 80 mmol m⁻² d⁻¹, thus exceeding the benthic oxygen uptake by about a factor of 8. The diapycnal flux profile exponentially decays with depth and the downward oxygen flux is reduced to less than 10 mmol m⁻² d⁻¹ at a depth of 60 m below the mixed layer. As the mixed layer depth averages to about 20 m, the diapycnal oxygen flux is able to completely supply the benthic oxygen uptake at water depths below 100 m. At about 150 m depth, however, the diapycnal flux changes sign due to the presence of the shallow OMZ and oxygen here is essentially fluxed upward, although at small rates. Thus, oxygen from the sea surface cannot contribute to ventilating the deeper water column via diapycnal mixing.

It should be noted that the diapycnal oxygen flux divergence from the mixed layer to 60 m below the mixed layer yields a diapycnal oxygen supply of about

On the role of circulation and mixing in the ventilation of OMZs

P. Brandt et al.

Title Page

Abstract

Introduction

Conclusions

References

Tables

Figures

⏪

⏩

◀

▶

Back

Close

Full Screen / Esc

Printer-friendly Version

Interactive Discussion



400 $\mu\text{mol kg}^{-1} \text{yr}^{-1}$. In steady state other oxygen transport processes and consumption are required to balance this substantial oxygen supply. While vertical advection during the upwelling season might contribute to the balance, the oxygen supply due to other transport processes should be at least an order of magnitude lower in this region.

5 The diapycnal oxygen supply to the upper thermocline can thus be used to define an upper limit of the oxygen consumption below the mixed layer. Such a consumption rate is, however, two orders of magnitude larger than the one estimated for the deep ocean as discussed above.

10 The results suggest that the high oxygen demand of the water column and the sediments within the upwelling region at shallow depths above the shallow OMZ may well be supplied from the surface via diapycnal mixing. Below that depth however, the continental slope must be ventilated via advective processes or isopycnal mixing. Nevertheless, although benthic oxygen uptake is an important local process decreasing oxygen levels in the bottom waters along the continental slope, it is negligible for the overall oxygen balance of the deep open ocean OMZ.

7 Long-term variability in ETNA OMZ

20 OMZs of the tropical oceans expanded and intensified during the last 50 years. Decreasing oxygen trends were found for the 300–700 m layers of selected regions with the strongest decrease in the ETNA of $-0.34 \pm 0.13 \mu\text{mol kg}^{-1} \text{yr}^{-1}$ for the region 10–14° N, 20–30° W (Stramma et al., 2008b). The global analysis of observed changes in the oxygen content between 1960–1974 and 1990–2008 indicates a widespread and significant deoxygenation at about 200 m depth in the tropical oceans (Stramma et al., 2010b). In the ETNA, this depth level corresponds to the intermediate oxygen maximum between the deep and shallow OMZs that is mainly ventilated by advection via zonal jets. A similar regional pattern of deoxygenation as for the 200 m level was found when vertically averaging oxygen changes over 200–700 m, albeit with a smaller amplitude (Stramma et al., 2010b).

with float data and model results, Czeschel et al. (2011) prepared a schematic on the intermediate circulation of the ETSP and its link to the OMZ. The centre of the OMZ is a stagnant flow area and the mean currents at 400 m depth in the open ocean ETSP are weak. Along the $\sim 86^\circ$ W section the lowest oxygen is observed between 6° S and 10° S centred at about 400 m depth and on the isopycnal $\sigma_\theta = 26.8 \text{ kg m}^{-3}$. Along this isopycnal the mean age is increased in the region of the low oxygen core with maximum mean age of about 300 yr at about 11° S, slightly poleward of the lowest oxygen concentration, and reduced near the equator with a mean age of about 200 yr (Fig. 20).

8.2 Mesoscale processes

Mesoscale variability occurs as linear Rossby waves and as nonlinear vortices or eddies. In contrast to linear waves, nonlinear vortices can transport momentum, heat, mass and the chemical constituents of seawater, and therefore contribute to the large scale water mass distribution (Chelton et al., 2007). Eddies move from the coastal upwelling regions westward and hence transport water offshore. These eddies affect the regions' biogeochemical budgets, but also the primary productivity of the regions (Lachkar and Gruber, 2012) and seem to play an important role for the oxygen distribution on the poleward side of the OMZ's. In global satellite observations of nonlinear mesoscale eddies by Chelton et al. (2011) it turned out that in the ETNA south and east of the Cape Verde Islands almost no eddies with a lifetime of ≥ 16 weeks were present, while in the ETSP a large number of such eddies could be identified, their occurrence extends close to the equator and the Peruvian shelf as can be seen in Fig. 4a of Chelton et al. (2011). Despite the inferred weak eddy activity in the ETNA, water mass anomalies including local oxygen minima at shallow depth just below the mixed layer have been found in cyclonic as well as in anticyclonic mode water eddies in this region (see Fig. 4, showing few profiles with oxygen concentration below $40 \mu\text{mol kg}^{-1}$). In the ETSP, a region of high eddy production is located just off the shelf at $15\text{--}16^\circ$ S and strong eddies were described from a survey in November 2012. A strong anticy-

On the role of circulation and mixing in the ventilation of OMZs

P. Brandt et al.

Title Page

Abstract

Introduction

Conclusions

References

Tables

Figures



Back

Close

Full Screen / Esc

Printer-friendly Version

Interactive Discussion



On the role of circulation and mixing in the ventilation of OMZs

P. Brandt et al.

Title Page

Abstract

Introduction

Conclusions

References

Tables

Figures

◀

▶

◀

▶

Back

Close

Full Screen / Esc

Printer-friendly Version

Interactive Discussion



the deep OMZ core, where it accounts for about one third of the oxygen supply required to balance consumption. There are, however, indications of regional variations in the diapycnal eddy diffusivity with higher values over the seamount region (up to one order of magnitude) compared to the abyssal plains (Fig. 11). The presence of seamounts in extended parts of ETNA OMZ might explain the observed smaller equatorward reduction of the diapycnal diffusivity than expected from internal wave-wave interaction theory (Heney et al., 1986; Gregg et al., 2003; Banyte et al., 2012). It might also be responsible for an increased diapycnal oxygen supply from below (Figs. 11 and 13).

The contribution of the mean advection to the oxygen budget cannot yet be quantified from observational data. The strength of the zonal jets penetrating into the ETNA OMZ (as well as into the ETSP OMZ) is of the order of a few cm s^{-1} and generally smaller than the characteristic eddy velocity (Hahn et al., 2014); the contribution of the zonal mean advection calculated from the currently available number of repeated ship sections remains thus uncertain. Note that the few moorings in the ETNA OMZ do not resolve the meridional structure of latitudinally stacked zonal jets. Instead, idealized advection–diffusion models were used to estimate the contribution of mean advection to the oxygen budget of the OMZ (Brandt et al., 2010, 2012). For these calculations a basin-wide mean velocity field has to be prescribed. However, the zonal extent of the zonal jets, their deviation from a purely zonal flow, and their connection to the well-ventilated western boundary regime are crucial in this calculation, but are not well constrained by observations, which leads again to a large uncertainty of the contribution of the mean advection to the oxygen budget of the ETNA OMZ.

Consumption as the main oxygen sink in the oxygen budget of the OMZ is currently best estimated as the net consumption along a water mass path from the subduction region toward the OMZ. The TTD concept additionally accounts for mixing between water masses following different paths (Haine and Hall, 2002; Karstensen et al., 2008; Schneider et al., 2012). Obtained net consumption estimates strongly depend on the water mass age and the comparison of different methods to derive such ages yields a range of possible consumption rates (Fig. 17). Besides this uncertainty, these esti-

be used, by including oxygen in the simulations, to study the roles of mean and variable advection in maintaining the tropical OMZs and to identify the mechanisms driving oxygen variability on interannual to multidecadal timescales.

The oxygen decline in the ETNA OMZ during the last decades corresponds to about 10% of the oxygen sink due to consumption not balanced by ventilation processes. This is a substantial imbalance in the oxygen budget of the ETNA OMZ. The regional pattern along the 23° W section indicates strongest oxygen reduction above the core of the deep OMZ and north of the Cape Verde archipelago (Fig. 18). Such a regional pattern is most likely associated with changes in the circulation pattern. Time series of all available oxygen data of the ETNA OMZ (Fig. 19) indicate variations on interannual, decadal, and multidecadal time scales; the long-term trend of deoxygenation associated with anthropogenic climate changes might not be the dominant signal on such a regional scale. Up to now, the regional pattern of observed oxygen changes cannot be reproduced by coupled climate-biogeochemistry models (Stramma et al., 2012), which could be the result of biases in the simulated mean circulation and oxygen distribution. Today it remains an open question how such biases influence the evolution of the oceanic oxygen content under on-going anthropogenic climate change in coupled climate-biogeochemistry simulations.

The oceanic oxygen distribution is sensitive to changes in the circulation. The observational program of the SFB 754 provides the possibility to acquire extended time series for studying interannual to decadal oxygen changes. Oxygen data from shipboard and moored observations show trend-like changes during the period 2006–2013 (Fig. 19) but also substantial interannual variability as for example associated with the EDJ (Fig. 8). The extension of these time series is essential to be able to test different hypotheses for the driving mechanisms of oxygen changes in the ocean. Using idealized or process models, distinct observed variability patterns might be reproduced and attributed to circulation changes and/or changes in the water mass distribution associated with the AMOC, STCs, PDO, or ENSO. For ocean circulation models the data

BGD

11, 12069–12136, 2014

On the role of circulation and mixing in the ventilation of OMZs

P. Brandt et al.

Title Page

Abstract

Introduction

Conclusions

References

Tables

Figures



Back

Close

Full Screen / Esc

Printer-friendly Version

Interactive Discussion



provide the basis for improving the physical system in coupled climate-biogeochemistry simulations to make projection of future oxygen evolution more reliable.

Acknowledgements. This study was funded by the Deutsche Forschungsgemeinschaft as part of the Sonderforschungsbereich 754 “Climate–Biogeochemistry Interactions in the Tropical Ocean”, through several research cruises with RV *Meteor* and RV *Maria S. Merian* and by the Deutsche Bundesministerium für Bildung und Forschung (BMBF) as part of the projects NORDATLANTIK (03F0443B), RACE (03F0651B), SOPRAN (03F0662A), and AWA (01DG12073E). Moored velocity and oxygen observations were partly acquired in cooperation with the PIRATA project and we would like to thank B. Boulès, R. Lumpkin, C. Schmid, and G. Foltz for their help with mooring work and data sharing. We also thank J. Lübbecke and L. D. Bryant for helpful discussions and comments on an earlier version of the manuscript. We thank the captains and crew of the RV *Maria S. Merian*, RV *Meteor*, and RV *L’Atalante* as well as our technical group for their help with the fieldwork.

The service charges for this open access publication have been covered by a Research Centre of the Helmholtz Association.

References

- Ascani, F., Firing, E., Dutrieux, P., McCreary, J. P., and Ishida, A.: Deep equatorial ocean circulation induced by a forced-dissipated Yanai beam, *J. Phys. Oceanogr.*, 40, 1118–1142, doi:10.1175/2010jpo4356.1, 2010.
- Banyte, D., Tanhua, T., Visbeck, M., Wallace, D. W. R., Karstensen, J., Krahnmann, G., Schneider, A., Stramma, L., and Dengler, M.: Diapycnal diffusivity at the upper boundary of the tropical North Atlantic oxygen minimum zone, *J. Geophys. Res.-Oceans*, 117, C09016, doi:10.1029/2011jc007762, 2012.
- Banyte, D., Visbeck, M., Tanhua, T., Fischer, T., Krahnmann, G., and Karstensen, J.: Lateral diffusivity from tracer release experiments in the tropical North Atlantic thermocline, *J. Geophys. Res.-Oceans*, 118, 2719–2733, doi:10.1002/Jgrc.20211, 2013.

On the role of circulation and mixing in the ventilation of OMZs

P. Brandt et al.

Title Page

Abstract

Introduction

Conclusions

References

Tables

Figures



Back

Close

Full Screen / Esc

Printer-friendly Version

Interactive Discussion



On the role of circulation and mixing in the ventilation of OMZs

P. Brandt et al.

[Title Page](#)

[Abstract](#)

[Introduction](#)

[Conclusions](#)

[References](#)

[Tables](#)

[Figures](#)



[Back](#)

[Close](#)

[Full Screen / Esc](#)

[Printer-friendly Version](#)

[Interactive Discussion](#)



- Barton, E. D.: The poleward undercurrent on the eastern boundary of the subtropical North Atlantic, in: Poleward Flows Along Eastern Ocean Boundaries, Lecture Note Series edn., edited by: Neshyba, S. J., Smith, R. L., and Mooers, C. N. K., Springer-Verlag, 82–95, 1989.
- Bianchi, D., Galbraith, E. D., Carozza, D. A., Mislán, K. A. S., and Stock, C. A.: Intensification of open-ocean oxygen depletion by vertically migrating animals, *Nat Geosci.*, 6, 545–548, doi:10.1038/Ngeo1837, 2013.
- Biastoch, A., Böning, C. W., Schwarzkopf, F. U., and Lutjeharms, J. R. E.: Increase in Agulhas leakage due to poleward shift of Southern Hemisphere westerlies, *Nature*, 462, 495–498, doi:10.1038/nature08519, 2009.
- Bolin, B. and Rodhe, H.: Note on concepts of age distribution and transit-time in natural reservoirs, *Tellus*, 25, 58–62, 1973.
- Bopp, L., Le Quere, C., Heimann, M., Manning, A. C., and Monfray, P.: Climate-induced oceanic oxygen fluxes: implications for the contemporary carbon budget, *Global Biogeochem. Cy.*, 16, 6-1–6-13, doi:10.1029/2001gb001445, 2002.
- Bourles, B., Lumpkin, R., McPhaden, M. J., Hernandez, F., Nobre, P., Campos, E., Yu, L. S., Planton, S., Busalacchi, A., Moura, A. D., Servain, J., and Trotte, J.: The PIRATA program: history, accomplishments, and future directions, *B. Am. Meteorol. Soc.*, 89, 1111–1125, doi:10.1175/2008bams2462.1, 2008.
- Brandt, P., Hormann, V., Bourles, B., Fischer, J., Schott, F. A., Stramma, L., and Dengler, M.: Oxygen tongues and zonal currents in the equatorial Atlantic, *J. Geophys. Res.-Oceans*, 113, C04012, doi:10.1029/2007jc004435, 2008.
- Brandt, P., Hormann, V., Körtzinger, A., Visbeck, M., Krahnemann, G., Stramma, L., Lumpkin, R., and Schmid, C.: Changes in the ventilation of the oxygen minimum zone of the tropical North Atlantic, *J. Phys. Oceanogr.*, 40, 1784–1801, doi:10.1175/2010jpo4301.1, 2010.
- Brandt, P., Funk, A., Hormann, V., Dengler, M., Greatbatch, R. J., and Toole, J. M.: Interannual atmospheric variability forced by the deep equatorial Atlantic Ocean, *Nature*, 473, 497–500, doi:10.1038/Nature10013, 2011.
- Brandt, P., Greatbatch, R. J., Claus, M., Didwischus, S. H., Hormann, V., Funk, A., Hahn, J., Krahnemann, G., Fischer, J., and Körtzinger, A.: Ventilation of the equatorial Atlantic by the equatorial deep jets, *J. Geophys. Res.-Oceans*, 117, C12015, doi:10.1029/2012jc008118, 2012.

On the role of circulation and mixing in the ventilation of OMZs

P. Brandt et al.

[Title Page](#)

[Abstract](#)

[Introduction](#)

[Conclusions](#)

[References](#)

[Tables](#)

[Figures](#)

[⏪](#)

[⏩](#)

[◀](#)

[▶](#)

[Back](#)

[Close](#)

[Full Screen / Esc](#)

[Printer-friendly Version](#)

[Interactive Discussion](#)



Canfield, D. E.: Organic Matter Oxidation in Marine Sediments, in: Interactions of C, N, P and S Biogeochemical Cycles and Global Change, edited by: Wollast, R., Mackenzie, F. T., and Chou, L., NATO ASI Series, Springer, Berlin, Heidelberg, 333–363, 1993.

Chaigneau, A., Dominguez, N., Eldin, G., Vasquez, L., Flores, R., Grados, C., and Echevin, V.: Near-coastal circulation in the Northern Humboldt Current System from shipboard ADCP data, *J. Geophys. Res.-Oceans*, 118, 5251–5266, doi:10.1002/Jgrc.20328, 2013.

Chang, P., Zhang, R., Hazeleger, W., Wen, C., Wan, X. Q., Ji, L., Haarsma, R. J., Breugem, W. P., and Seidel, H.: Oceanic link between abrupt changes in the North Atlantic Ocean and the African monsoon, *Nat. Geosci.*, 1, 444–448, doi:10.1038/Ngeo218, 2008.

Chelton, D. B., Schlax, M. G., Samelson, R. M., and de Szoeke, R. A.: Global observations of large oceanic eddies, *Geophys Res Lett.*, 34, L15606, doi:10.1029/2007gl030812, 2007.

Chelton, D. B., Schlax, M. G., and Samelson, R. M.: Global observations of nonlinear mesoscale eddies, *Prog Oceanogr.*, 91, 167–216, doi:10.1016/J.Pocean.2011.01.002, 2011.

Czeschel, R., Stramma, L., Schwarzkopf, F. U., Giese, B. S., Funk, A., and Karstensen, J.: Middepth circulation of the eastern tropical South Pacific and its link to the oxygen minimum zone, *J. Geophys. Res.-Oceans*, 116, C01015, doi:10.1029/2010jc006565, 2011.

Czeschel, R., Stramma, L., and Johnson, G. C.: Oxygen decreases and variability in the eastern equatorial Pacific, *J. Geophys. Res.-Oceans*, 117, C11019, doi:10.1029/2012jc008043, 2012.

d'Orgeville, M., Hua, B. L., and Sasaki, H.: Equatorial deep jets triggered by a large vertical scale variability within the western boundary layer, *J. Mar. Res.*, 65, 1–25, doi:10.1357/002224007780388720, 2007.

Dale, A. W., Sommer, S., Ryabenko, E., Noffke, A., Bohlen, L., Wallmann, K., Stolpovsky, K., Greinert, J., and Pfannkuche, O.: Benthic nitrogen fluxes and fractionation of nitrate in the Mauritanian oxygen minimum zone (Eastern Tropical North Atlantic), *Geochim Cosmochim Acta.*, 134, 234–256, doi:10.1016/J.Gca.2014.02.026, 2014.

Davis, R. E.: Intermediate-depth circulation of the Indian and South Pacific Oceans measured by autonomous floats, *J. Phys. Oceanogr.*, 35, 683–707, doi:10.1175/Jpo2702.1, 2005.

Duteil, O., Schwarzkopf, F. U., Böning, C. W., and Oschlies, A.: Major role of the equatorial current system in setting oxygen levels in the eastern tropical Atlantic Ocean: a high-resolution model study, *Geophys. Res. Lett.*, 41, 2033–2040, doi:10.1002/2013gl058888, 2014.

Eden, C.: Eddy length scales in the North Atlantic Ocean, *J. Geophys. Res.-Oceans*, 112, C06004, doi:10.1029/2006jc003901, 2007.

On the role of circulation and mixing in the ventilation of OMZs

P. Brandt et al.

Title Page

Abstract

Introduction

Conclusions

References

Tables

Figures

◀

▶

◀

▶

Back

Close

Full Screen / Esc

Printer-friendly Version

Interactive Discussion



- Eden, C. and Greatbatch, R. J.: A diagnosis of isopycnal mixing by mesoscale eddies, *Ocean Model.*, 27, 98–106, doi:10.1016/j.ocemod.2008.12.002, 2009.
- Ferrari, R. and Polzin, K. L.: Finescale structure of the T-S relation in the eastern North Atlantic, *J. Phys. Oceanogr.*, 35, 1437–1454, doi:10.1175/Jpo2763.1, 2005.
- 5 Fischer, T., Banyte, D., Brandt, P., Dengler, M., Krahnemann, G., Tanhua, T., and Visbeck, M.: Diapycnal oxygen supply to the tropical North Atlantic oxygen minimum zone, *Biogeosciences*, 10, 5079–5093, doi:10.5194/bg-10-5079-2013, 2013.
- Frölicher, T. L., Joos, F., Plattner, G. K., Steinacher, M., and Doney, S. C.: Natural variability and anthropogenic trends in oceanic oxygen in a coupled carbon cycle-climate model ensemble, *Global Biogeochem. Cy.*, 23, GB1003, doi:10.1029/2008gb003316, 2009.
- 10 Glud, R. N.: Oxygen dynamics of marine sediments, *Mar. Biol. Res.*, 4, 243–289, doi:10.1080/17451000801888726, 2008.
- Gnanadesikan, A., Bianchi, D., and Pradal, M. A.: Critical role for mesoscale eddy diffusion in supplying oxygen to hypoxic ocean waters, *Geophys. Res. Lett.*, 40, 5194–5198, doi:10.1002/Grl.50998, 2013.
- 15 Gregg, M. C., Sanford, T. B., and Winkel, D. P.: Reduced mixing from the breaking of internal waves in equatorial waters, *Nature*, 422, 513–515, doi:10.1038/Nature01507, 2003.
- Hagen, E.: Northwest African upwelling scenario, *Oceanol. Acta*, 24, 113–128, doi:10.1016/S0399-1784(00)01110-5, 2001.
- 20 Hahn, J., Brandt, P., Greatbatch, R. J., Krahnemann, G., and Körtzinger, A.: Oxygen variance and meridional oxygen supply in the Tropical North East Atlantic oxygen minimum zone, *Clim. Dynam.*, in press, 1–26, doi:10.1007/s00382-014-2065-0, 2014.
- Haine, T. W. N. and Hall, T. M.: A generalized transport theory: water-mass composition and age, *J. Phys. Oceanogr.*, 32, 1932–1946, doi:10.1175/1520-0485(2002)032<1932:Agttwm>2.0.Co;2, 2002.
- 25 Helm, K. P., Bindoff, N. L., and Church, J. A.: Observed decreases in oxygen content of the global ocean, *Geophys. Res. Lett.*, 38, L23602, doi:10.1029/2011gl049513, 2011.
- Henyey, F. S., Wright, J., and Flatte, S. M.: Energy and action flow through the internal wave field – an Eikonal approach, *J. Geophys. Res.-Oceans*, 91, 8487–8495, doi:10.1029/Jc091ic07p08487, 1986.
- 30 Holloway, P. E.: A comparison of semidiurnal internal tides from different bathymetric locations on the Australian North-West Shelf, *J. Phys. Oceanogr.*, 15, 240–251, doi:10.1175/1520-0485(1985)015<0240:Acosit>2.0.Co;2, 1985.

On the role of circulation and mixing in the ventilation of OMZs

P. Brandt et al.

Title Page

Abstract

Introduction

Conclusions

References

Tables

Figures



Back

Close

Full Screen / Esc

Printer-friendly Version

Interactive Discussion



Holtappels, M., Tiano, L., Kalvelage, T., Lavik, G., Revsbech, N. P., and Kuypers, M. M. M.: Aquatic respiration rate measurements at low oxygen concentrations, *Plos One*, 9, e89369, doi:10.1371/journal.pone.0089369, 2014.

Hua, B. L., d'Orgeville, M., Fruman, M. D., Menesguen, C., Schopp, R., Klein, P., and Sasaki, H.: Destabilization of mixed Rossby gravity waves and the formation of equatorial zonal jets, *J. Fluid. Mech.*, 610, 311–341, doi:10.1017/S0022112008002656, 2008.

Jenkins, W. J.: Oxygen utilization rates in North-Atlantic sub-tropical gyre and primary production in oligotrophic systems, *Nature*, 300, 246–248, doi:10.1038/300246a0, 1982.

Jenkins, W. J.: Studying subtropical thermocline ventilation and circulation using tritium and He-3, *J. Geophys. Res.-Oceans*, 103, 15817–15831, doi:10.1029/98jc00141, 1998.

Jochum, M., Malanotte-Rizzoli, P., and Busalacchi, A.: Tropical instability waves in the Atlantic ocean, *Ocean. Model.*, 7, 145–163, doi:10.1016/S1463-5003(03)00042-8, 2004.

Kamenkovich, I., Berloff, P., and Pedlosky, J.: Anisotropic material transport by eddies and eddy-driven currents in a model of the North Atlantic, *J. Phys. Oceanogr.*, 39, 3162–3175, doi:10.1175/2009jpo4239.1, 2009.

Karstensen, J., Stramma, L., and Visbeck, M.: Oxygen minimum zones in the eastern tropical Atlantic and Pacific oceans, *Prog. Oceanogr.*, 77, 331–350, doi:10.1016/J.Pocean.2007.05.009, 2008.

Keeling, R. F. and Garcia, H. E.: The change in oceanic O-2 inventory associated with recent global warming, *P. Natl. Acad. Sci. USA*, 99, 7848–7853, doi:10.1073/Pnas.122154899, 2002.

Keeling, R. F., Körtzinger, A., and Gruber, N.: Ocean deoxygenation in a warming world, *Annu. Rev. Mar. Sci.*, 2, 199–229, doi:10.1146/Annurev.Marine.010908.163855, 2010.

Kessler, W. S.: The circulation of the eastern tropical Pacific: a review, *Prog. Oceanogr.*, 69, 181–217, doi:10.1016/J.Pocean.2006.03.009, 2006.

Kirchner, K., Rhein, M., Hüttl-Kabus, S., and Böning, C. W.: On the spreading of South Atlantic Water into the Northern Hemisphere, *J. Geophys. Res.-Oceans*, 114, C05019, doi:10.1029/2008JC005165, 2009.

Lachkar, Z. and Gruber, N.: A comparative study of biological production in eastern boundary upwelling systems using an artificial neural network, *Biogeosciences*, 9, 293–308, doi:10.5194/bg-9-293-2012, 2012.

Ledwell, J. R., Watson, A. J., and Law, C. S.: Mixing of a tracer in the pycnocline, *J. Geophys. Res.-Oceans*, 103, 21499–21529, doi:10.1029/98jc01738, 1998.

On the role of circulation and mixing in the ventilation of OMZs

P. Brandt et al.

Title Page

Abstract

Introduction

Conclusions

References

Tables

Figures

◀

▶

◀

▶

Back

Close

Full Screen / Esc

Printer-friendly Version

Interactive Discussion



Lu, Z. T., Schlosser, P., Smethie Jr, W. M., Sturchio, N. C., Fischer, T. P., Kennedy, B. M., Purtschert, R., Severinghaus, J. P., Solomon, D. K., Tanhua, T., and Yokochi, R.: Tracer applications of noble gas radionuclides in the geosciences, *Earth-Sci. Rev.*, in press, doi:10.1016/j.earscirev.2013.09.002, 2014.

5 Lutz, M., Dunbar, R., and Caldeira, K.: Regional variability in the vertical flux of particulate organic carbon in the ocean interior, *Global Biogeochem. Cy.*, 16, 1037, doi:10.1029/2000gb001383, 2002.

Luyten, J., Pedlosky, J., and Stommel, H.: Climatic Inferences from the Ventilated Thermocline, *Climatic Change*, 5, 183–191, doi:10.1007/Bf00141269, 1983a.

10 Luyten, J. R., Pedlosky, J., and Stommel, H.: The ventilated thermocline, *J. Phys. Oceanogr.*, 13, 292–309, doi:10.1175/1520-0485(1983)013<0292:Tvt>2.0.Co;2, 1983b.

Machin, F. and Pelegri, J. L.: Northward penetration of Antarctic Intermediate Water off North-west Africa, *J. Phys. Oceanogr.*, 39, 512–535, doi:10.1175/2008jpo3825.1, 2009.

15 Malanotte-Rizzoli, P., Hedstrom, K., Arango, H., and Haidvogel, D. B.: Water mass pathways between the subtropical and tropical ocean in a climatological simulation of the North Atlantic ocean circulation, *Dynam. Atmos. Oceans*, 32, 331–371, doi:10.1016/S0377-0265(00)00051-8, 2000.

Martin, J. H., Knauer, G. A., Karl, D. M., and Broenkow, W. W.: Vertex – carbon cycling in the Northeast Pacific, *Deep-Sea Res. Pt. I*, 34, 267–285, doi:10.1016/0198-0149(87)90086-0, 1987.

20 Martz, T. R., Johnson, K. S., and Riser, S. C.: Ocean metabolism observed with oxygen sensors on profiling floats in the South Pacific, *Limnol. Oceanogr.*, 53, 2094–2111, doi:10.4319/Lo.2008.53.5_Part_2.2094, 2008.

25 Matear, R. J. and Hirst, A. C.: Long-term changes in dissolved oxygen concentrations in the ocean caused by protracted global warming, *Global Biogeochem. Cy.*, 17, 1125, doi:10.1029/2002gb001997, 2003.

Maximenko, N. A., Bang, B., and Sasaki, H.: Observational evidence of alternating zonal jets in the world ocean, *Geophys. Res. Lett.*, 32, doi:10.1029/2005gl022728, 2005.

30 McCreary, J. P., Yu, Z. J., Hood, R. R., Vinayachandran, P. N., Furue, R., Ishida, A., and Richards, K. J.: Dynamics of the Indian-Ocean oxygen minimum zones, *Prog. Oceanogr.*, 112, 15–37, doi:10.1016/J.Pocean.2013.03.002, 2013.

On the role of circulation and mixing in the ventilation of OMZs

P. Brandt et al.

Title Page

Abstract

Introduction

Conclusions

References

Tables

Figures

◀

▶

◀

▶

Back

Close

Full Screen / Esc

Printer-friendly Version

Interactive Discussion

- Ménesguen, C., Hua, B. L., Fruman, M. D., and Schopp, R.: Dynamics of the combined extra-equatorial and equatorial deep jets in the Atlantic, *J. Mar. Res.*, 67, 323–346, doi:10.1357/002224009789954766, 2009.
- Mittelstaedt, E.: The upwelling area off Northwest Africa – a description of phenomena related to coastal upwelling, *Prog. Oceanogr.*, 12, 307–331, doi:10.1016/0079-6611(83)90012-5, 1983.
- Mittelstaedt, E.: The ocean boundary along the Northwest African Coast – circulation and oceanographic properties at the sea-surface, *Prog Oceanogr.*, 26, 307–355, doi:10.1016/0079-6611(91)90011-A, 1991.
- Ollitrault, M., Lankhorst, M., Fratantoni, D., Richardson, P., and Zenk, W.: Zonal intermediate currents in the equatorial Atlantic Ocean, *Geophys. Res. Lett.*, 33, L05605, doi:10.1029/2005gl025368, 2006.
- Oschlies, A., Schulz, K. G., Riebesell, U., and Schmittner, A.: Simulated 21st century's increase in oceanic suboxia by CO₂-enhanced biotic carbon export, *Global Biogeochem. Cy.*, 22, GB4008, doi:10.1029/2007gb003147, 2008.
- Pena-Izquierdo, J., Pelegri, J. L., Pastor, M. V., Castellanos, P., Emelianov, M., Gasser, M., Salvador, J., and Vazquez-Dominguez, E.: The continental slope current system between Cape Verde and the Canary Islands, *Sci. Mar.*, 76, 65–78, doi:10.3989/Scimar.03607.18c, 2012.
- Plattner, G. K., Joos, F., and Stocker, T. F.: Revision of the global carbon budget due to changing air–sea oxygen fluxes, *Global Biogeochem. Cy.*, 16, 1096, doi:10.1029/2001gb001746, 2002.
- Qiu, B., Chen, S. M., and Sasaki, H.: Generation of the North Equatorial Undercurrent jets by triad baroclinic Rossby wave interactions, *J. Phys. Oceanogr.*, 43, 2682–2698, doi:10.1175/Jpo-D-13-099.1, 2013.
- Rabe, B., Schott, F. A., and Kohl, A.: Mean circulation and variability of the tropical Atlantic during 1952–2001 in the GECCO assimilation fields, *J. Phys. Oceanogr.*, 38, 177–192, doi:10.1175/2007jpo3541.1, 2008.
- Riley, G. A.: Oxygen, phosphate, and nitrate in the Atlantic Ocean, *Bull. Bingham. Oceanogr. Coll.*, 12, 1–126, 1951.
- Roether, W., Jean-Baptiste, P., Fourné, E., and Sültenfuß, J.: The transient distributions of nuclear weapon-generated tritium and its decay product ³He in the Mediterranean Sea,

On the role of circulation and mixing in the ventilation of OMZs

P. Brandt et al.

Title Page

Abstract

Introduction

Conclusions

References

Tables

Figures

◀

▶

◀

▶

Back

Close

Full Screen / Esc

Printer-friendly Version

Interactive Discussion



1952–2011, and their oceanographic potential, *Ocean Sci.*, 9, 837–854, doi:10.5194/os-9-837-2013, 2013.

Sandstrom, H., and Oakey, N. S.: Dissipation in internal tides and solitary waves, *J. Phys. Oceanogr.*, 25, 604–614, doi:10.1175/1520-0485(1995)025<0604:Diitas>2.0.Co;2, 1995.

Schafstall, J., Dengler, M., Brandt, P., and Bange, H.: Tidal-induced mixing and diapycnal nutrient fluxes in the Mauritanian upwelling region, *J. Geophys. Res.-Oceans*, 115, C10014, doi:10.1029/2009jc005940, 2010.

Schmidtko, S., Johnson, G. C., and Lyman, J. M.: MIMOC: a global monthly isopycnal upper-ocean climatology with mixed layers, *J. Geophys. Res.-Oceans*, 118, 1658–1672, doi:10.1002/Jgrc.20122, 2013.

Schmittner, A., Oschlies, A., Matthews, H. D., and Galbraith, E. D.: Future changes in climate, ocean circulation, ecosystems, and biogeochemical cycling simulated for a business-as-usual CO₂ emission scenario until year 4000 AD, *Global Biogeochem Cy.*, 22, GB1013, doi:10.1029/2007gb002953, 2008.

Schneider, A., Tanhua, T., Körtzinger, A., and Wallace, D. W. R.: An evaluation of tracer fields and anthropogenic carbon in the equatorial and the tropical North Atlantic, *Deep-Sea Res. Pt. I*, 67, 85–97, doi:10.1016/J.Dsr.2012.05.007, 2012.

Schott, F. A., Stramma, L., and Fischer, J.: The warm water inflow into the western tropical Atlantic boundary regime, spring 1994, *J. Geophys. Res.-Oceans*, 100, 24745–24760, doi:10.1029/95jc02803, 1995.

Schott, F. A., Fischer, J., and Stramma, L.: Transports and pathways of the upper-layer circulation in the western tropical Atlantic, *J. Phys. Oceanogr.*, 28, 1904–1928, doi:10.1175/1520-0485(1998)028<1904:TAPOTU>2.0.CO;2, 1998.

Schott, F. A., McCreary, J. P., and Johnson, G. C.: Shallow overturning circulations of the tropical-subtropical oceans, in: *Earth Climate: the Ocean–Atmosphere Interaction*, edited by: Wang, C., Xie, S.-P., and Carton, J. A., *Geophysical Monograph 147*, American Geophysical Union, Washington, DC, 261–304, 2004.

Schott, F. A., Dengler, M., Zantopp, R., Stramma, L., Fischer, J., and Brandt, P.: The shallow and deep western boundary circulation of the South Atlantic at 5°–11° S, *J. Phys. Oceanogr.*, 35, 2031–2053, doi:10.1175/JPO2813.1, 2005.

St Laurent, L., and Schmitt, R. W.: The contribution of salt fingers to vertical mixing in the North Atlantic Tracer Release Experiment, *J. Phys. Oceanogr.*, 29, 1404–1424, doi:10.1175/1520-0485(1999)029<1404:Tcosft>2.0.Co;2, 1999.

On the role of circulation and mixing in the ventilation of OMZs

P. Brandt et al.

Title Page

Abstract

Introduction

Conclusions

References

Tables

Figures



Back

Close

Full Screen / Esc

Printer-friendly Version

Interactive Discussion



Stanley, R. H. R., Doney, S. C., Jenkins, W. J., and Lott III, D. E.: Apparent oxygen utilization rates calculated from tritium and helium-3 profiles at the Bermuda Atlantic Time-series Study site, *Biogeosciences*, 9, 1969–1983, doi:10.5194/bg-9-1969-2012, 2012.

Stendardo, I., and Gruber, N.: Oxygen trends over five decades in the North Atlantic, *J. Geophys. Res.-Oceans*, 117, C11004, doi:10.1029/2012jc007909, 2012.

Stramma, L. and England, M. H.: On the water masses and mean circulation of the South Atlantic Ocean, *J. Geophys. Res.-Oceans*, 104, 20863–20883, doi:10.1029/1999JC900139, 1999.

Stramma, L., Brandt, P., Schafstall, J., Schott, F., Fischer, J., and Körtzinger, A.: Oxygen minimum zone in the North Atlantic south and east of the Cape Verde Islands, *J. Geophys. Res.-Oceans*, 113, doi:10.1029/2007jc004369, 2008a.

Stramma, L., Johnson, G. C., Sprintall, J., and Mohrholz, V.: Expanding oxygen-minimum zones in the tropical oceans, *Science*, 320, 655–658, doi:10.1126/science.1153847, 2008b.

Stramma, L., Visbeck, M., Brandt, P., Tanhua, T., and Wallace, D.: Deoxygenation in the oxygen minimum zone of the eastern tropical North Atlantic, *Geophys. Res. Lett.*, 36, L20607, doi:10.1029/2009gl039593, 2009.

Stramma, L., Johnson, G. C., Firing, E., and Schmidtko, S.: Eastern Pacific oxygen minimum zones: supply paths and multidecadal changes, *J. Geophys. Res.-Oceans*, 115, C09011, doi:10.1029/2009jc005976, 2010a.

Stramma, L., Schmidtko, S., Levin, L. A., and Johnson, G. C.: Ocean oxygen minima expansions and their biological impacts, *Deep-Sea Res. Pt. I*, 57, 587–595, doi:10.1016/J.Dsr.2010.01.005, 2010b.

Stramma, L., Oschlies, A., and Schmidtko, S.: Mismatch between observed and modeled trends in dissolved upper-ocean oxygen over the last 50 yr, *Biogeosciences*, 9, 4045–4057, doi:10.5194/bg-9-4045-2012, 2012.

Stramma, L., Bange, H. W., Czeschel, R., Lorenzo, A., and Frank, M.: On the role of mesoscale eddies for the biological productivity and biogeochemistry in the eastern tropical Pacific Ocean off Peru, *Biogeosciences*, 10, 7293–7306, doi:10.5194/bg-10-7293-2013, 2013.

Stramma, L., Weller, R. A., Czeschel, R., and Bigorre, S.: Eddies and an extreme water mass anomaly observed in the eastern south Pacific at the Stratus mooring, *J. Geophys. Res. Oceans*, 119, 2169–9291, doi:10.1002/2013JC009470, 2014.

**On the role of
circulation and
mixing in the
ventilation of OMZs**P. Brandt et al.

[Title Page](#)[Abstract](#)[Introduction](#)[Conclusions](#)[References](#)[Tables](#)[Figures](#)[Back](#)[Close](#)[Full Screen / Esc](#)[Printer-friendly Version](#)[Interactive Discussion](#)

Suga, T. and Talley, L. D.: Antarctic intermediate water circulation in the tropical and subtropical South-Atlantic, *J. Geophys. Res.-Oceans*, 100, 13441–13453, doi:10.1029/95jc00858, 1995.

Sverdrup, H. U.: On the Explanation of the Oxygen Minima and Maxima in the Oceans, *J. Conseil*, 13, 163–172, doi:10.1093/icesjms/13.2.163, 1938.

Tatebe, H., Imada, Y., Mori, M., Kimoto, M., and Hasumi, H.: Control of decadal and bidecadal climate variability in the tropical Pacific by the off-equatorial South Pacific Ocean, *J. Climate*, 26, 6524–6534, doi:10.1175/Jcli-D-12-00137.1, 2013.

Thiele, G. and Sarmiento, J. L.: Tracer dating and ocean ventilation, *J. Geophys. Res.-Oceans*, 95, 9377–9391, doi:10.1029/Jc095ic06p09377, 1990.

Tsuchiya, M.: Thermostats and circulation in the upper layer of the Atlantic Ocean, *Prog. Oceanogr.*, 16, 235–267, 1986.

Tsuchiya, M., Talley, L. D., and McCartney, M. S.: An eastern Atlantic section from Iceland southward across the equator, *Deep-Sea Res. Pt. I*, 39, 1885–1917, doi:10.1016/0198-0149(92)90004-D, 1992.

von Schuckmann, K., Brandt, P., and Eden, C.: Generation of tropical instability waves in the Atlantic Ocean, *J. Geophys. Res.-Oceans*, 113, C08034, doi:10.1029/2007jc004712, 2008.

Wattenberg, H.: Die Verteilung des Sauerstoffs im Atlantischen Ozean, *Wissenschaftliche Ergebnisse der Deutschen Atlantischen Expedition auf dem Forschungs- und Vermessungsschiff Meteor 1925–1927*, 9.1, edited by: Defant, A., de Gruyter, Berlin, Leipzig, 132 pp., 1938.

Waugh, D. W., Haine, T. W. N., and Hall, T. M.: Transport times and anthropogenic carbon in the subpolar North Atlantic Ocean, *Deep-Sea Res. Pt. I*, 51, 1475–1491, doi:10.1016/J.Dsr.2004.06.011, 2004.

Weiss, R. F.: Solubility of nitrogen, oxygen and argon in water and seawater, *Deep-Sea Res.*, 17, 721–735, doi:10.1016/0011-7471(70)90037-9, 1970.

Wollast, R.: Evaluation and comparison of the global carbon cycle in the coastal zone and in the open ocean, in: *The Sea*, edited by: Robinson, A. and Brink, K. H., Wiley, New York, 213–252, 1998.

Wüst, G.: Die Stratosphäre des Atlantischen Ozeans, *Deutsche Atlantische Exped. Meteor 1925–1927*, *Wiss. Erg.*, 6, 288 pp., 1935.

Wyrki, K.: The oxygen minima in relation to ocean circulation, *Deep-Sea Res.*, 9, 11–23, doi:10.1016/0011-7471(62)90243-7, 1962.

Table 1. SFB 754 research cruises to the tropical eastern Atlantic and Pacific oceans.

Vessel and Cruise (Date)	Main Work	Region
Tropical Atlantic, 5° S–14° N/23° W		
L'Atalante GEOMAR 4 (Feb–Mar 2008)	23° W section, moorings	2° S–14° N
Maria S. Merian 08/1 (Apr–May 2008)	GUTRE tracer release	23° W, 8° N at 300 m
Maria S. Merian 10/1 (Nov–Dec 2008)	GUTRE tracer survey	4–14° N/27.5–17.5° W
Meteor 80/1 (Oct–Nov 2009)	23° W section, moorings	5° S–14° N
Meteor 80/2 (Dec 2009)	GUTRE tracer survey	4–14° N/31–15° W
Meteor 83/1 (Oct–Nov 2010)	GUTRE tracer survey	2–15° N/28–15° W
Maria S. Merian 18/2 (May–Jun 2011)	23° W section, moorings	5° S–14° N
Maria S. Merian 18/3 (Jun–Jul 2011)	23° W section	4–14° N
Maria S. Merian 22 (Oct–Nov 2012)	23° W section, moorings	5° S–14° N/23° W
Maria S. Merian 23 (Dec 2012)	OSTRE tracer release	21° W, 11° N at 500 m
Tropical Atlantic, 26° W–16° W/18° N		
L'Atalante GEOMAR 3 (Feb 2008)	18° N section	24.3–16.3° W
Maria S. Merian 22 (Nov 2012)	18° N section	26–19.7° W
Tropical Pacific, 22° S–2° N/~ 86° W		
Meteor 77/3 (Jan 2009)	Continental slope	18–10° S
Meteor 77/4 (Feb 2009)	~ 86° W section	14° S–2° N
Meteor 90 (Nov 2012)	~ 86° W section	22° S–2° N
Meteor 92 (Jan 2013)	Continental slope	13–10° S
Meteor 93 (Feb 2013)	Continental slope	14–10° S

On the role of circulation and mixing in the ventilation of OMZs

P. Brandt et al.

Title Page

Abstract

Introduction

Conclusions

References

Tables

Figures

◀

▶

◀

▶

Back

Close

Full Screen / Esc

Printer-friendly Version

Interactive Discussion



On the role of circulation and mixing in the ventilation of OMZs

P. Brandt et al.

Table 2. SFB 754 subsurface moorings in the eastern tropical Atlantic.

Position	Period	Parameters	Depth [m]
0°/23° W	May 2011–Oct 2012	u O ₂	20–720 300, 500
5° N/23° W	Nov 2009–Oct 2012	u T, S, O ₂	60–780 100–800
8° N/23° W	Nov 2009–Oct 2012	u T, S, O ₂	60–750 100–800

Title Page

Abstract

Introduction

Conclusions

References

Tables

Figures



Back

Close

Full Screen / Esc

Printer-friendly Version

Interactive Discussion



On the role of circulation and mixing in the ventilation of OMZs

P. Brandt et al.

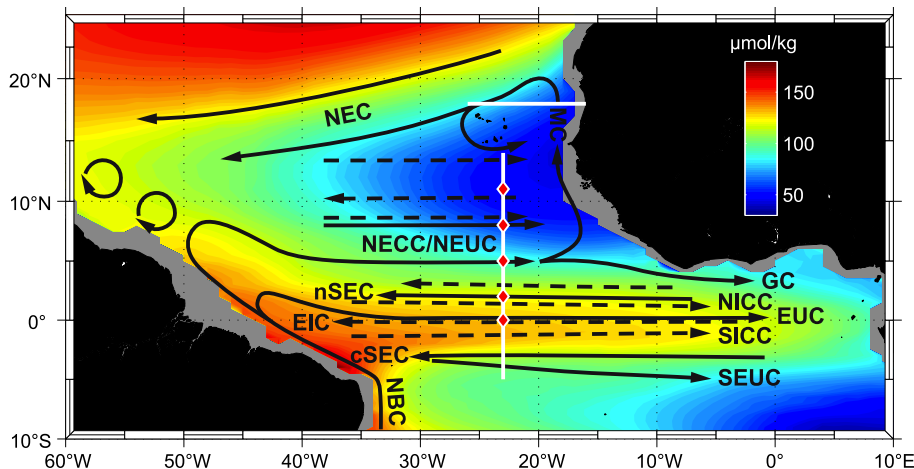


Figure 1. Oxygen concentration [$\mu\text{mol kg}^{-1}$] in the tropical Atlantic at $\sigma_\theta = 27.1 \text{ kg m}^{-3}$ (close to the deep oxygen minimum) as obtained from the MIMOC climatology (Schmidtko et al., 2013) with circulation schematic superimposed. Surface and thermocline current branches shown (black solid arrows) are the North Equatorial Current (NEC), the Mauritania Current (MC), the northern and central branch of the South Equatorial Current (nSEC and cSEC), the North Equatorial Countercurrent (NECC), the Guinea Current (GC), the North Brazil Current (NBC), the North and South Equatorial Undercurrent (NEUC and SEUC), and the Equatorial Undercurrent (EUC). Intermediate current branches shown (black dashed arrows) are North and South Intermediate Countercurrents (NICC and SICC) or “flanking jets”, and the Equatorial Intermediate Current (EIC). The 23° W and 18° N repeat sections are marked by white lines, mooring positions by red diamonds.

Title Page

Abstract

Introduction

Conclusions

References

Tables

Figures

◀

▶

◀

▶

Back

Close

Full Screen / Esc

Printer-friendly Version

Interactive Discussion



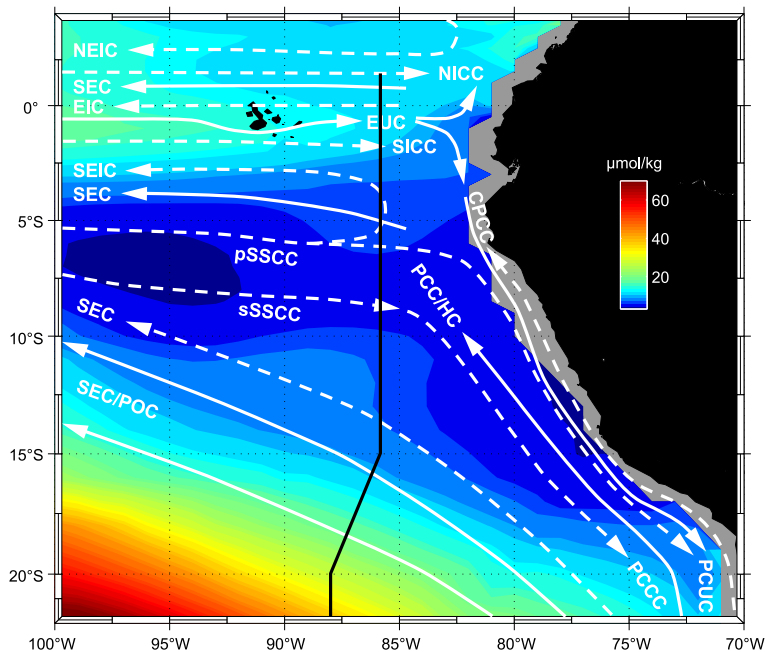


Figure 2. Oxygen concentration [$\mu\text{mol kg}^{-1}$] in the eastern tropical Pacific at $\sigma_{\theta} = 26.8 \text{ kg m}^{-3}$ (close to the deep oxygen minimum) as obtained from the MIMOC climatology (Schmidtko et al., 2013) with circulation schematic superimposed. Current bands displayed are for the surface layer (white solid arrows) the South Equatorial Current (SEC), the Equatorial Undercurrent (EUC), the Peru–Chile or Humboldt Current (PCC/HC), the Peru Oceanic Current (POC) and for the thermocline layer (white dashed arrows) the North Equatorial Intermediate Current (NEIC), the North Intermediate Countercurrent (NICC), the Equatorial Intermediate Current (EIC), the South Intermediate Countercurrent (pSSCC, sSSCC), the deeper layer of the SEC, the Chile–Peru Coastal Current (CPCC), the Peru–Chile Undercurrent (PCUC) and the Peru–Chile Countercurrent (PCCC). The location of the $\sim 86^{\circ}\text{W}$ section is marked as black line.

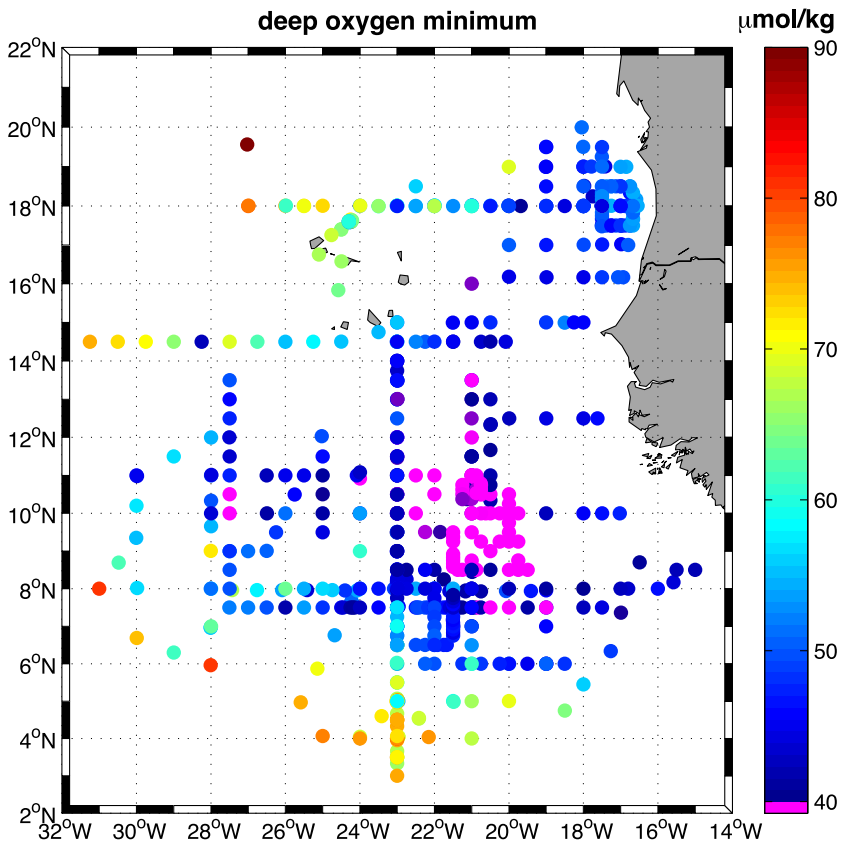


Figure 3. Oxygen concentration at the deep oxygen minimum (below 200 m) as obtained from CTD station data taken during the period 2006 to 2013. Oxygen concentration below $40 \mu\text{mol kg}^{-1}$ is marked by purple dots.

Title Page	
Abstract	Introduction
Conclusions	References
Tables	Figures
◀	▶
◀	▶
Back	Close
Full Screen / Esc	
Printer-friendly Version	
Interactive Discussion	



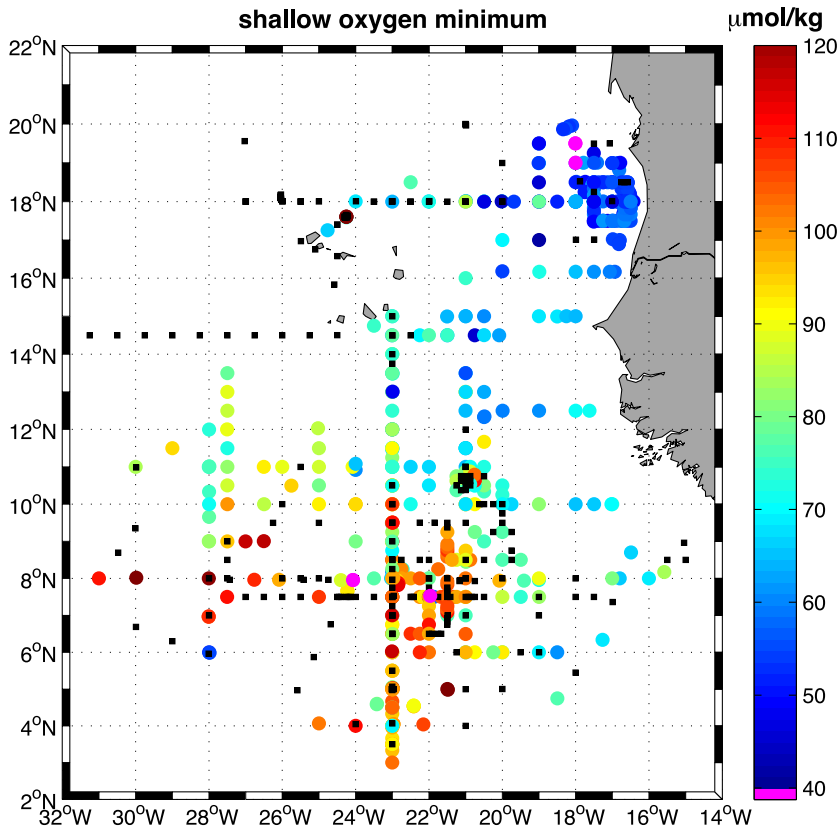


Figure 4. Oxygen concentration at the shallow oxygen minimum (above 200 m) as obtained from CTD station data taken during the period 2006 to 2013. Black squares indicate profiles without a shallow oxygen minimum (i.e. minimum oxygen of the upper 200 m was at about 200 m). Oxygen concentration below $40 \mu\text{mol kg}^{-1}$ is marked by purple dots.

On the role of circulation and mixing in the ventilation of OMZs

P. Brandt et al.

[Title Page](#)

[Abstract](#) | [Introduction](#)

[Conclusions](#) | [References](#)

[Tables](#) | [Figures](#)

[◀](#) | [▶](#)

[◀](#) | [▶](#)

[Back](#) | [Close](#)

[Full Screen / Esc](#)

[Printer-friendly Version](#)

[Interactive Discussion](#)



On the role of circulation and mixing in the ventilation of OMZs

P. Brandt et al.

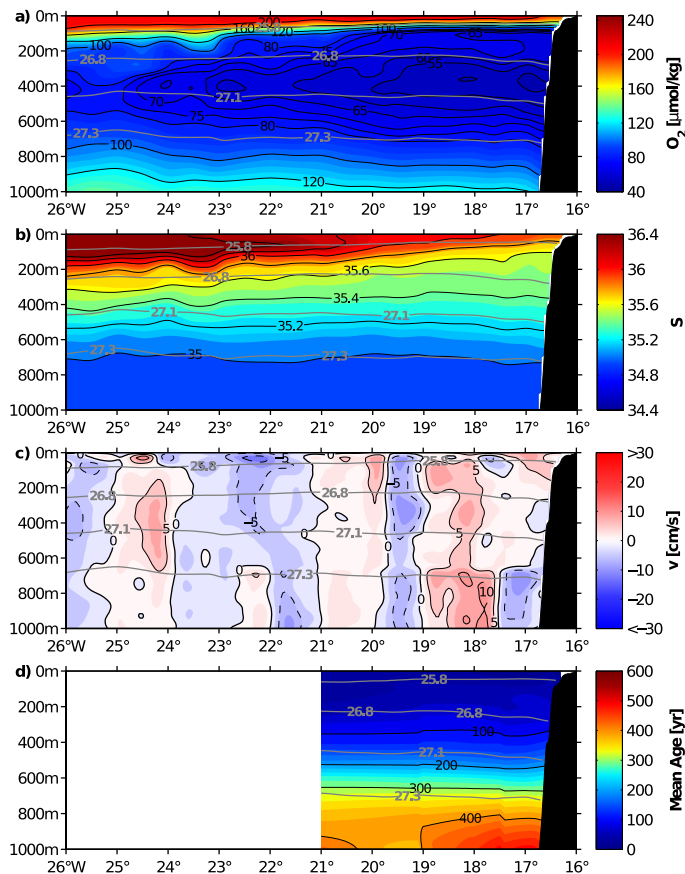


Figure 5. (a) Mean oxygen content, (b) salinity, (c) meridional velocity (positive northward), and (d) mean age as obtained from zonal ship sections taken along 18° N during 2005–2012. Grey contours mark potential density [kg m^{-3}]. Besides the deep oxygen minimum at about 400 m depth there is a shallow oxygen minimum at about 100 m in proximity to the shelf (a).

Title Page

Abstract

Introduction

Conclusions

References

Tables

Figures

◀

▶

◀

▶

Back

Close

Full Screen / Esc

Printer-friendly Version

Interactive Discussion



On the role of circulation and mixing in the ventilation of OMZs

P. Brandt et al.

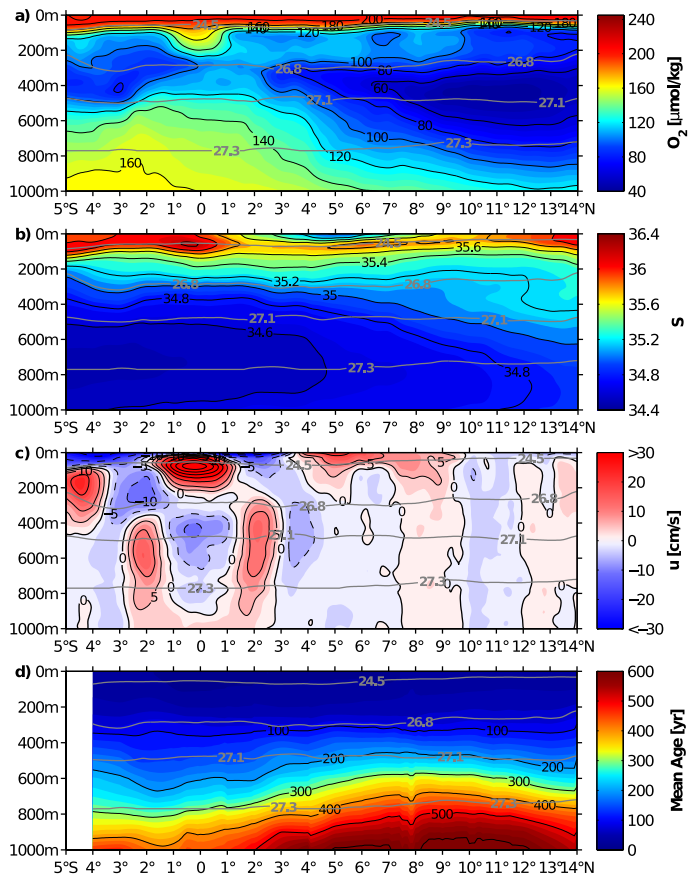


Figure 6. (a) Mean oxygen content, (b) salinity, (c) zonal velocity (positive eastward), and (d) mean age as obtained from meridional ship sections taken along 23°W during 1999–2012. Grey contours mark potential density [kg m^{-3}]. Eastward current bands, marked by reddish colours, are generally associated with elevated oxygen content.

Title Page

Abstract

Introduction

Conclusions

References

Tables

Figures

◀

▶

◀

▶

Back

Close

Full Screen / Esc

Printer-friendly Version

Interactive Discussion



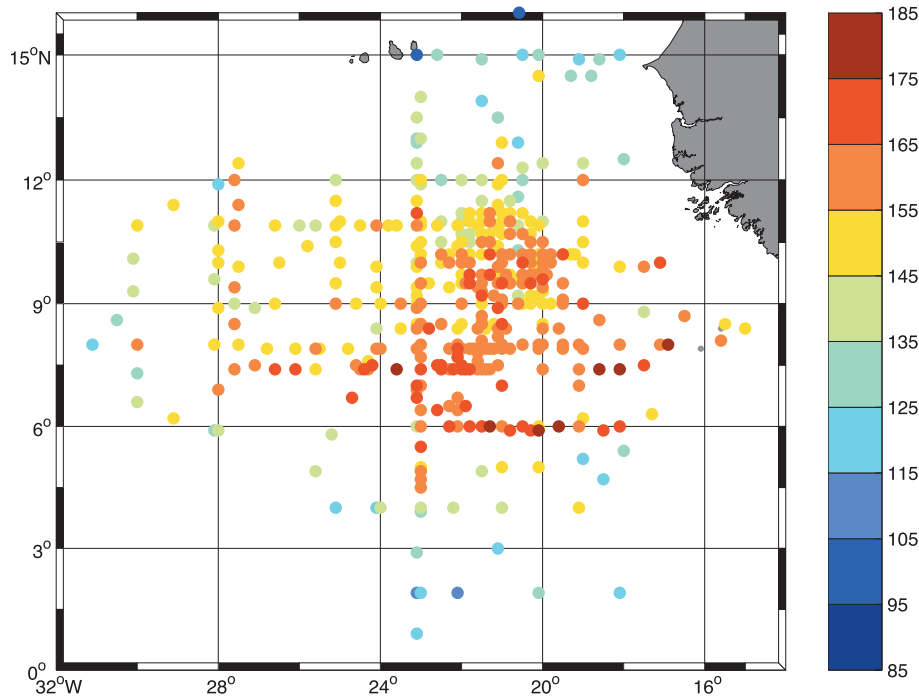


Figure 7. Mean age [yr] at $\sigma_{\theta} = 27.0 \text{ kg m}^{-3}$ which corresponds approximately to the depth of the deep oxygen minimum.

On the role of circulation and mixing in the ventilation of OMZs

P. Brandt et al.

Title Page	
Abstract	Introduction
Conclusions	References
Tables	Figures
◀	▶
◀	▶
Back	Close
Full Screen / Esc	
Printer-friendly Version	
Interactive Discussion	



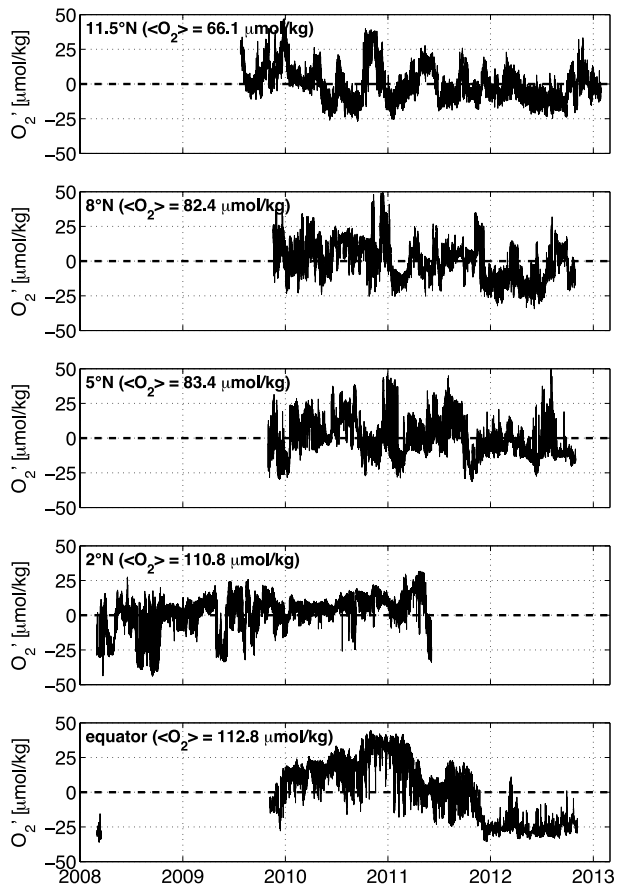


Figure 8. Time series of oxygen anomaly at about 300 m depth from moored observations along 23° W at different latitudes. Mean oxygen values at the different mooring locations are given in brackets.

On the role of circulation and mixing in the ventilation of OMZs

P. Brandt et al.

[Title Page](#)

[Abstract](#) | [Introduction](#)

[Conclusions](#) | [References](#)

[Tables](#) | [Figures](#)

[◀](#) | [▶](#)

[◀](#) | [▶](#)

[Back](#) | [Close](#)

[Full Screen / Esc](#)

[Printer-friendly Version](#)

[Interactive Discussion](#)



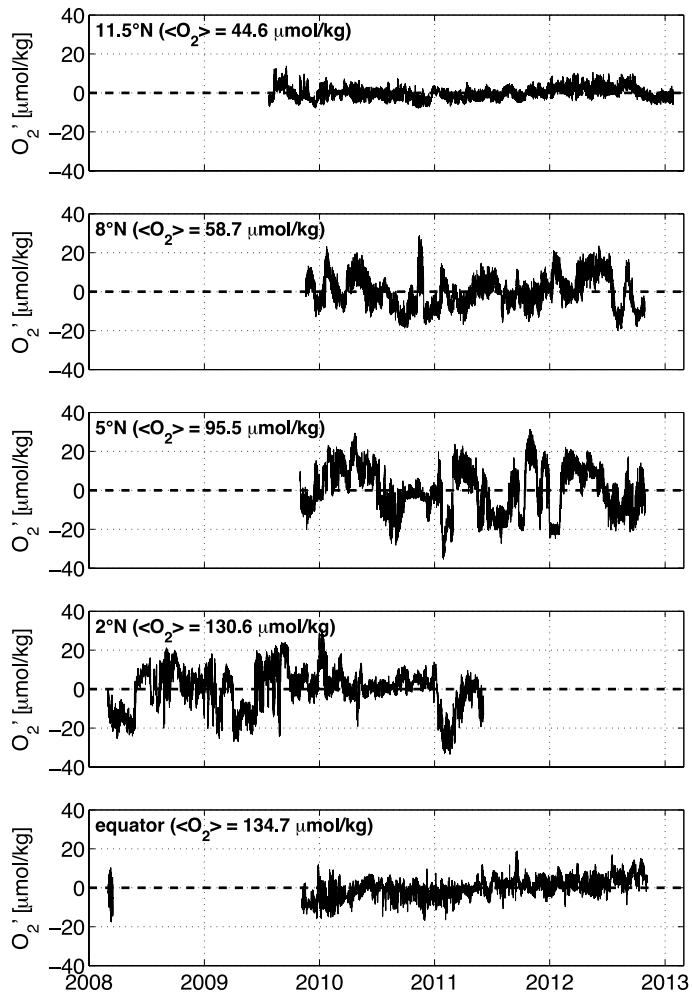


Figure 9. As Fig. 8, but at about 500 m depth.

12124

On the role of circulation and mixing in the ventilation of OMZs

P. Brandt et al.

Title Page	
Abstract	Introduction
Conclusions	References
Tables	Figures
◀	▶
◀	▶
Back	Close
Full Screen / Esc	
Printer-friendly Version	
Interactive Discussion	



On the role of circulation and mixing in the ventilation of OMZs

P. Brandt et al.

Title Page

Abstract

Introduction

Conclusions

References

Tables

Figures

◀

▶

◀

▶

Back

Close

Full Screen / Esc

Printer-friendly Version

Interactive Discussion

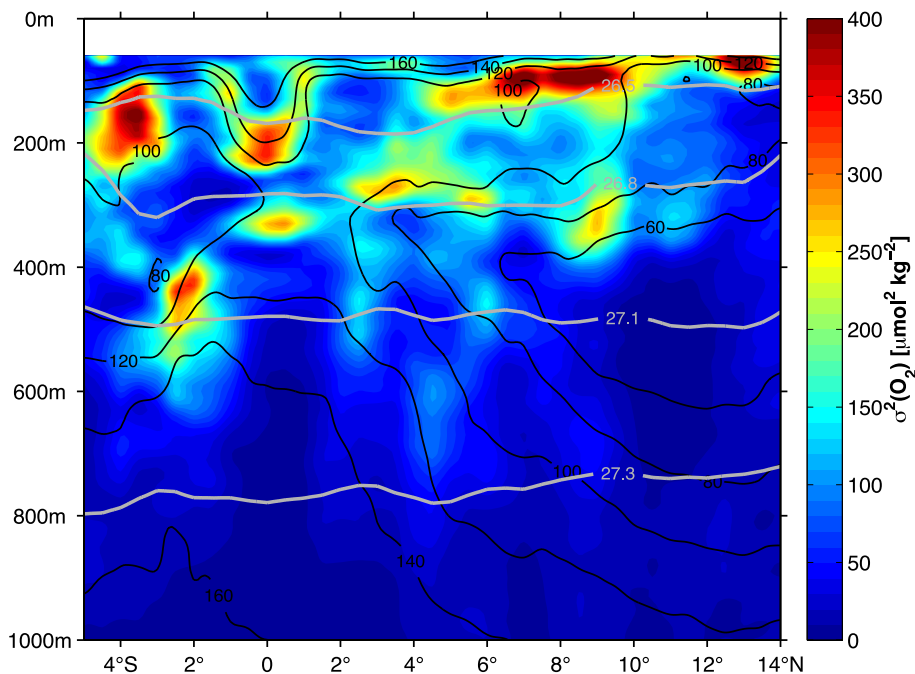


Figure 10. Oxygen variance along 23°W from repeat ship sections. The analysis was done on isopycnal surfaces and the results were projected back onto depth coordinates. Grey contours mark potential density [kg m^{-3}], black contours mark mean oxygen [$\mu\text{mol kg}^{-1}$].

On the role of circulation and mixing in the ventilation of OMZs

P. Brandt et al.

Title Page

Abstract

Introduction

Conclusions

References

Tables

Figures

◀

▶

◀

▶

Back

Close

Full Screen / Esc

Printer-friendly Version

Interactive Discussion

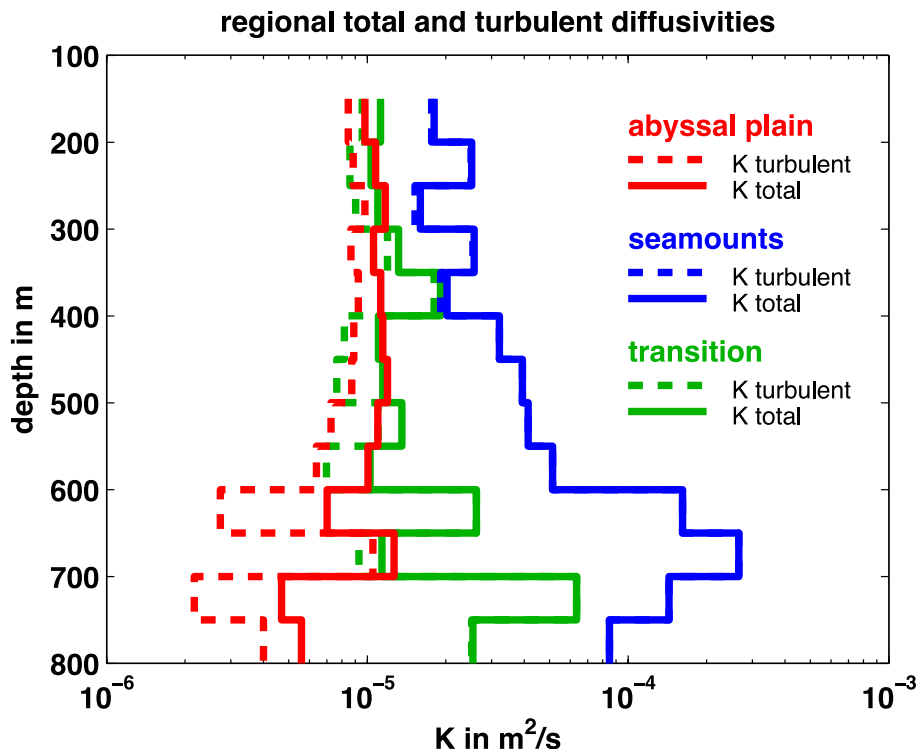


Figure 11. Profiles of the diapycnal eddy diffusivity as estimated from microstructure measurements (dashed lines) and by accounting for the effect of double diffusion (solid lines) for different regions: (red) abyssal plain, (blue) seamount region, and (green) transition region.

On the role of circulation and mixing in the ventilation of OMZs

P. Brandt et al.

[Title Page](#)

[Abstract](#)

[Introduction](#)

[Conclusions](#)

[References](#)

[Tables](#)

[Figures](#)

[◀](#)

[▶](#)

[◀](#)

[▶](#)

[Back](#)

[Close](#)

[Full Screen / Esc](#)

[Printer-friendly Version](#)

[Interactive Discussion](#)

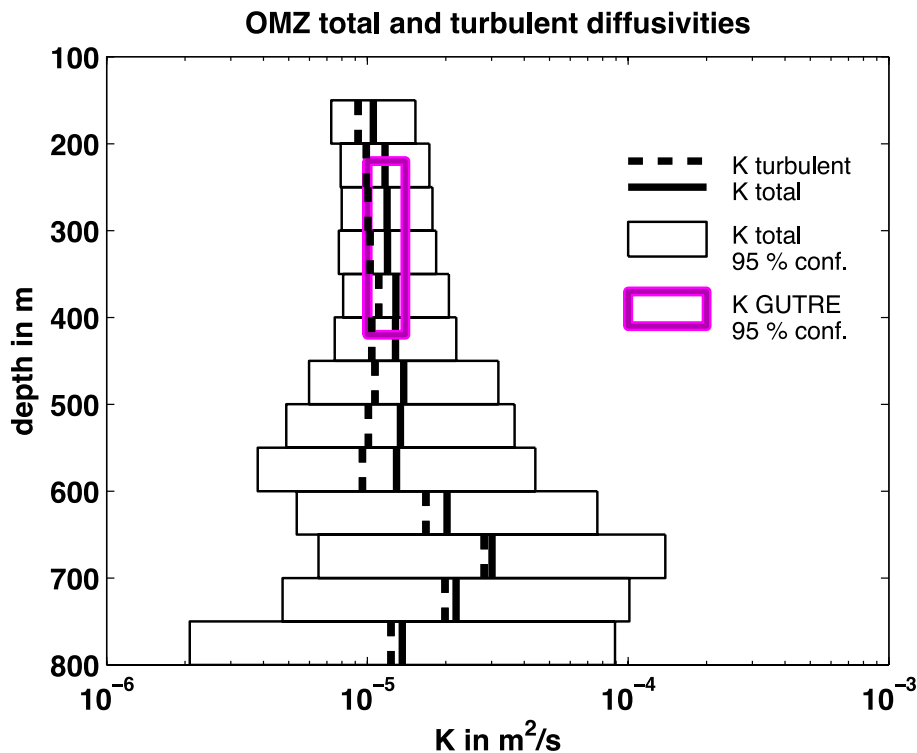


Figure 12. Diapycnal eddy diffusivity as estimated from microstructure measurements (dashed black line) and the tracer release experiment (purple box representing 95 % confidence error level). The profile of total diapycnal eddy diffusivity is obtained by accounting for the effect of double diffusion (solid black line with 95 % confidence error level).

On the role of circulation and mixing in the ventilation of OMZs

P. Brandt et al.

Title Page

Abstract

Introduction

Conclusions

References

Tables

Figures

◀

▶

◀

▶

Back

Close

Full Screen / Esc

Printer-friendly Version

Interactive Discussion

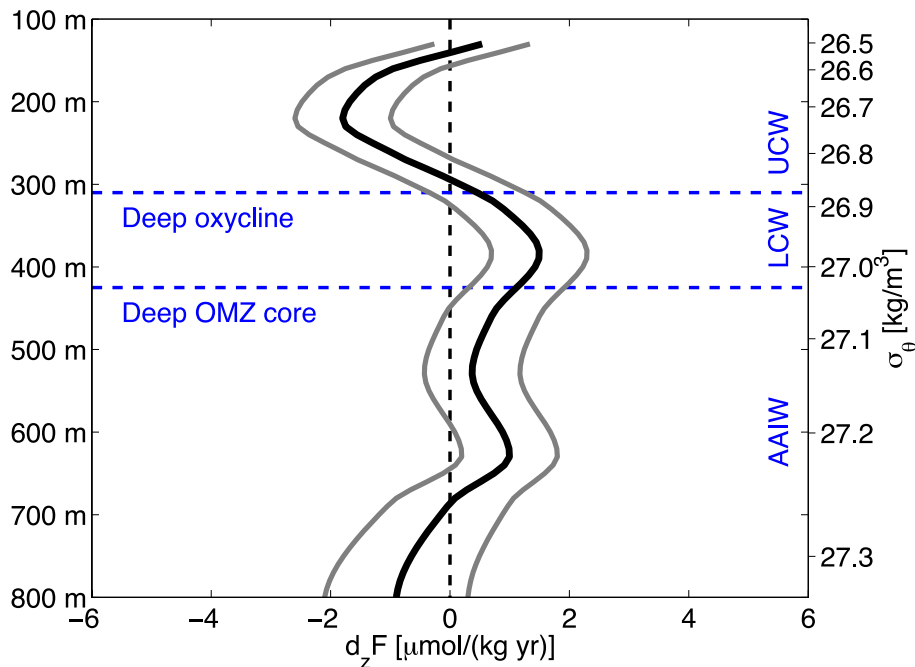


Figure 13. Mean oxygen supply due to diapycnal mixing (solid black line) for the open ocean ETNA OMZ and 95 % confidence error level (solid grey lines) as function of depth (left axis) or potential density (right axis). Blue dashed lines mark the depths of the deep oxycline and of the core of the deep OMZ that separate layers of upper and lower CW, and AAIW.

On the role of circulation and mixing in the ventilation of OMZs

P. Brandt et al.

Title Page

Abstract

Introduction

Conclusions

References

Tables

Figures

◀

▶

◀

▶

Back

Close

Full Screen / Esc

Printer-friendly Version

Interactive Discussion

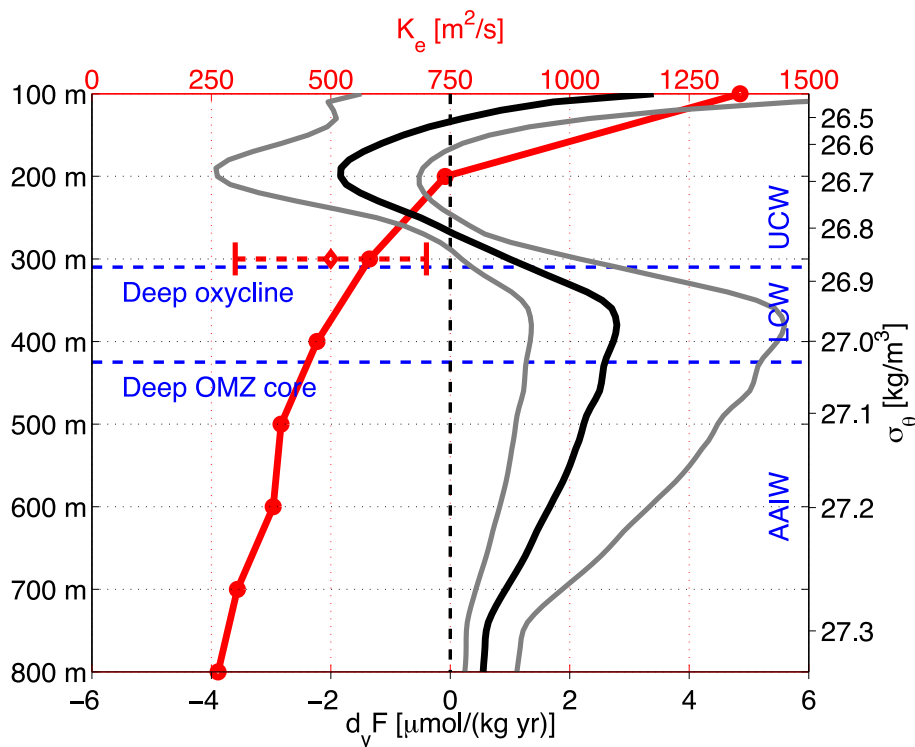


Figure 14. Eddy diffusivity as estimated from moored and shipboard observations (red circles, red line, upper axis) and from the tracer release experiment (red diamond with error bar, upper axis) as function of depth (left axis) or potential density (right axis). Also shown is the mean isopycnal meridional eddy-driven oxygen supply (black line, lower axis) for the open ocean ETNA OMZ with 95 % confidence error levels (grey lines, lower axis; see further details in text and in Hahn et al., 2014). Blue dashed lines mark the depths of the deep oxycline and of the core of the deep OMZ that separate layers of upper and lower CW, and AAIW.

On the role of circulation and mixing in the ventilation of OMZs

P. Brandt et al.

Title Page

Abstract

Introduction

Conclusions

References

Tables

Figures

◀

▶

◀

▶

Back

Close

Full Screen / Esc

Printer-friendly Version

Interactive Discussion

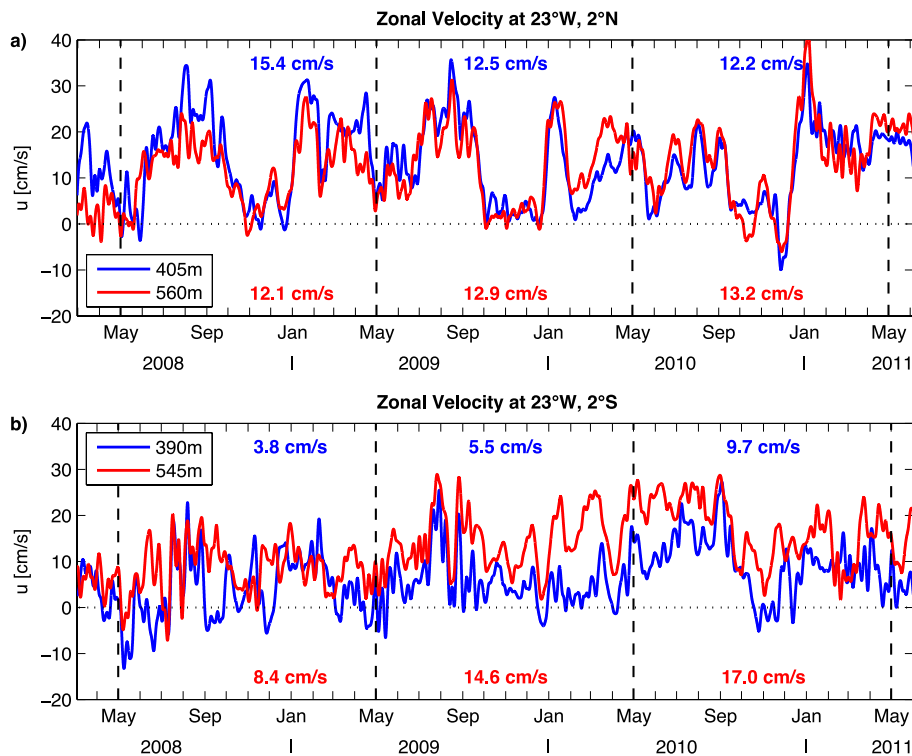


Figure 15. Zonal velocity from moored observations at 23° W, 2° N **(a)** and 23° W, 2° S **(b)** at about 400 m (blue lines) and 550 m (red lines). Blue and red numbers represent annual mean velocities at about 400 m and 550 m depth, respectively. Dashed vertical lines mark time periods used for the calculation of annual means; dotted horizontal line marks zero velocity.

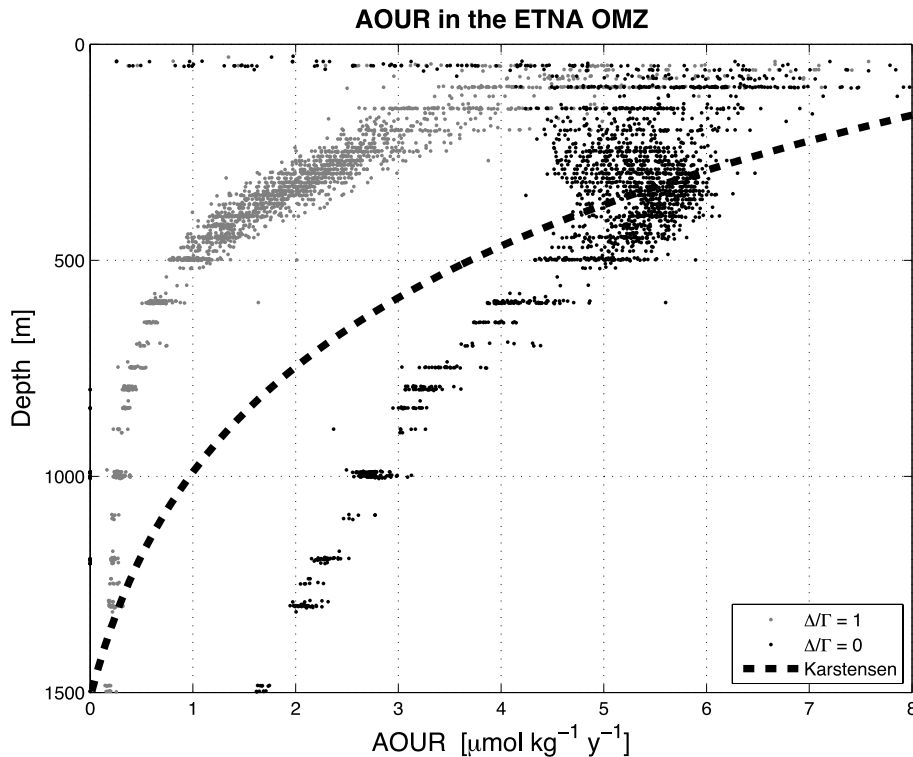


Figure 16. AOUR in the ETNA OMZ (between 4° N and 14° N and east of 32° W). The AOUR was calculated using the TTD approach with two different assumptions about mixing: black dots corresponds to no mixing, $\Delta/\Gamma = 0$; grey dots to moderate mixing, $\Delta/\Gamma = 1$. The dashed line marks AOUR as obtained by Karstensen et al. (2008) using CFC-11 ages from the ventilated gyre.

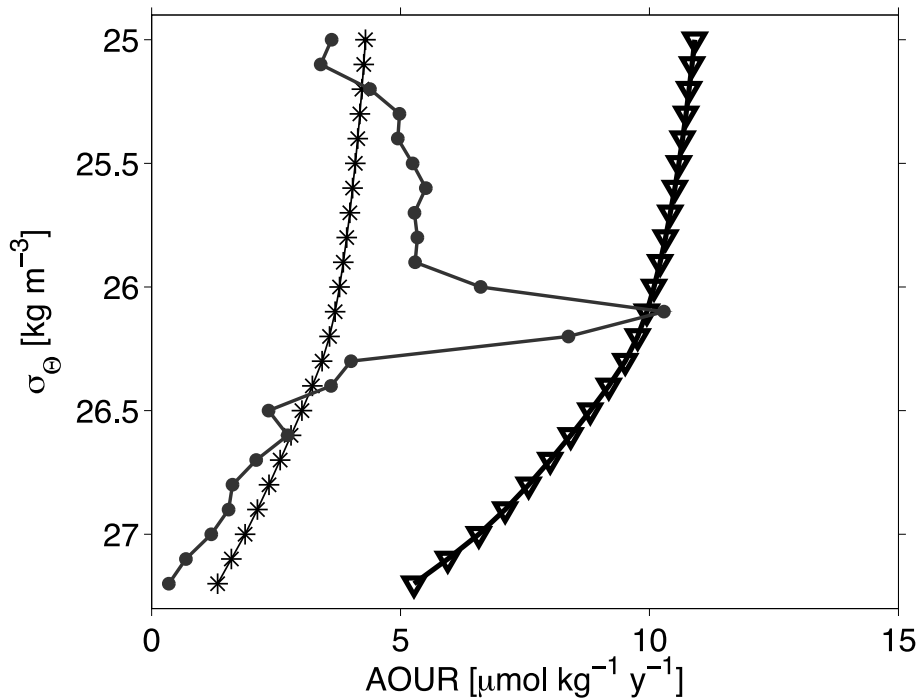


Figure 17. AOUR as function of density as obtained by Schneider et al. (2012) using the TTD approach for the ETNA (stars) and by Karstensen et al. (2008) using CFC-11 ages from the ventilated gyre (triangles), and using the ratio of North Atlantic (0–60° N) basin scale mean AOU for discrete density increments of 0.1 kg m^{-3} and respective reservoir ages (black dots, see further details, e.g. reservoir ages and volumes, in Karstensen et al., 2008).

On the role of circulation and mixing in the ventilation of OMZs

P. Brandt et al.

Title Page

Abstract

Introduction

Conclusions

References

Tables

Figures

◀

▶

◀

▶

Back

Close

Full Screen / Esc

Printer-friendly Version

Interactive Discussion

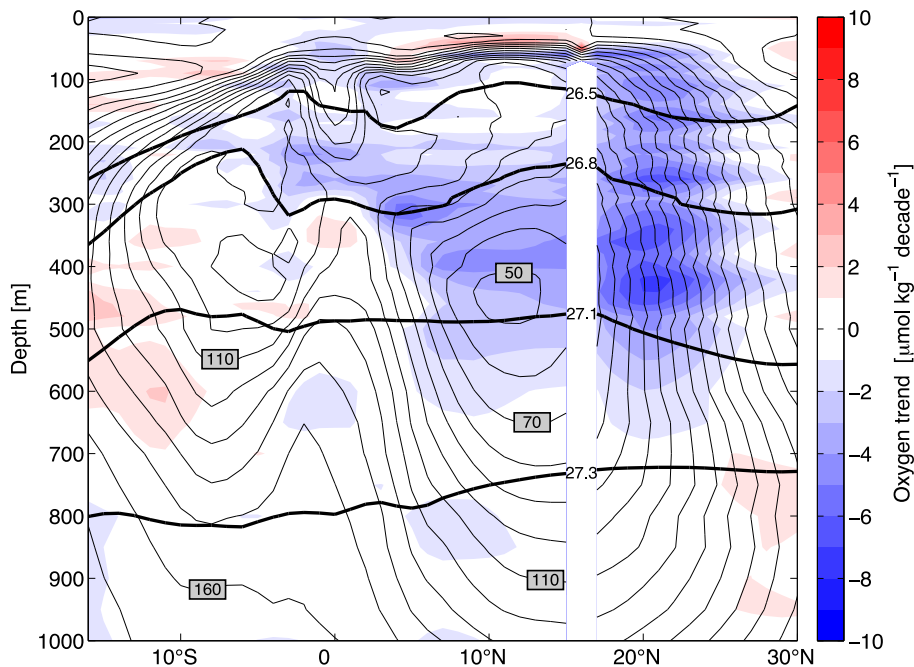


Figure 18. Oxygen trend along 23° W between 20° W and 26° W and between 1972 and 2013 as obtained from the MIMOC climatology (Schmidtke et al., 2013). The trend was calculated on depth coordinates using oxygen anomalies relative to mean oxygen. Thin black contours mark mean oxygen [$\mu\text{mol kg}^{-1}$], thick black contours mark potential density [kg m^{-3}], both from the MIMOC climatology.

On the role of circulation and mixing in the ventilation of OMZs

P. Brandt et al.

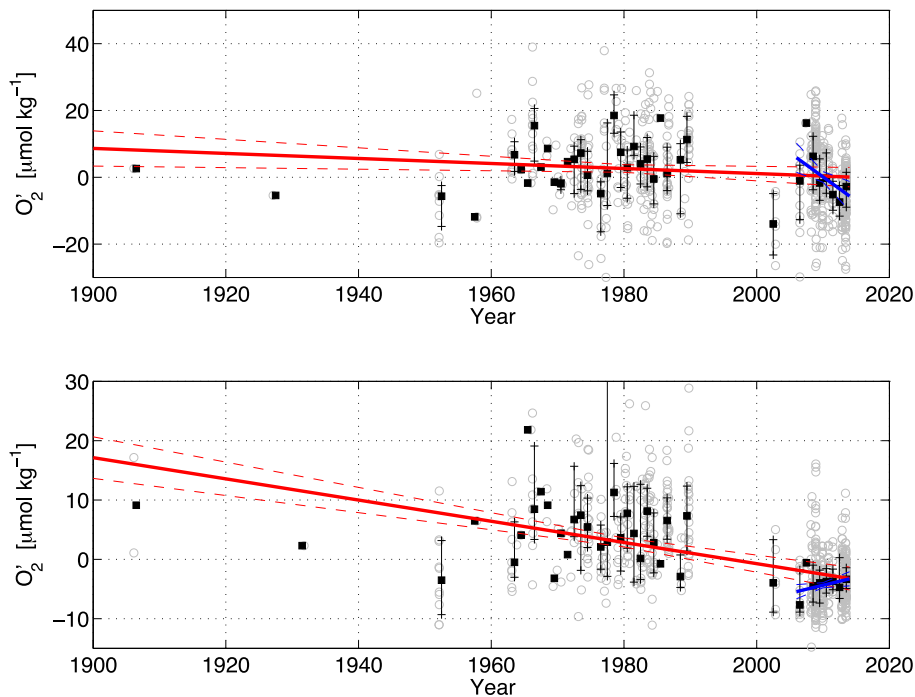


Figure 19. Oxygen anomalies for the region 9–15° N, 20–26° W and 150–300 m (intermediate oxygen maximum, upper panel) and 350–700 m (deep oxygen minimum, lower panel). Grey circles represent all available data, whiskers show interquartile range of data within each year and the black squares annual medians. Trends are calculated using annual medians weighted by the square root of available data within each year for the period 1900–2013 (solid red line) and 2006–2013 (solid blue line). The dashed lines mark the standard errors of the trends.

Title Page

Abstract

Introduction

Conclusions

References

Tables

Figures

◀

▶

◀

▶

Back

Close

Full Screen / Esc

Printer-friendly Version

Interactive Discussion



On the role of circulation and mixing in the ventilation of OMZs

P. Brandt et al.

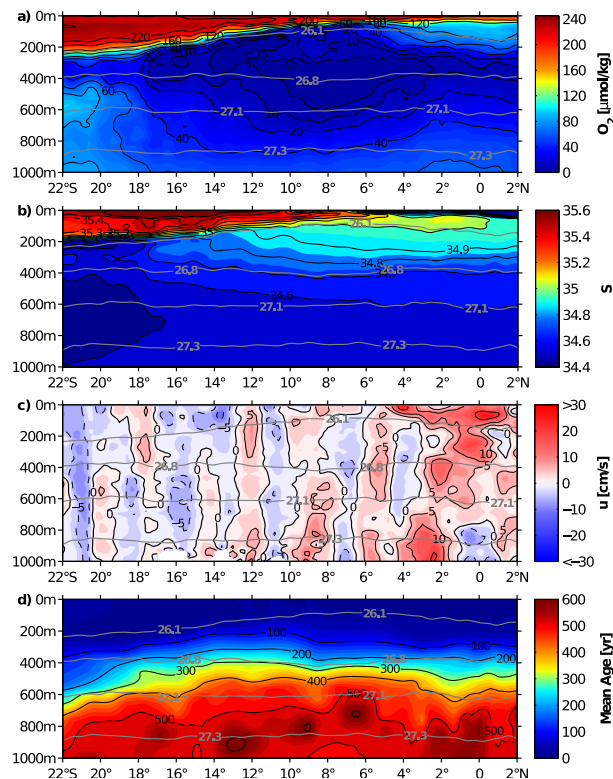


Figure 20. (a) Mean oxygen content, (b) salinity, (c) zonal velocity (positive eastward), and (d) mean age as obtained from meridional ship sections taken on three Pacific surveys along $\sim 86^\circ$ W during 1993–2012. Grey contours mark potential density [kg m^{-3}]. The mean age is solely based on data from 1993. Eastward current bands, marked by reddish colours, are generally associated with elevated oxygen content.

Title Page

Abstract

Introduction

Conclusions

References

Tables

Figures

◀

▶

◀

▶

Back

Close

Full Screen / Esc

Printer-friendly Version

Interactive Discussion

On the role of circulation and mixing in the ventilation of OMZs

P. Brandt et al.

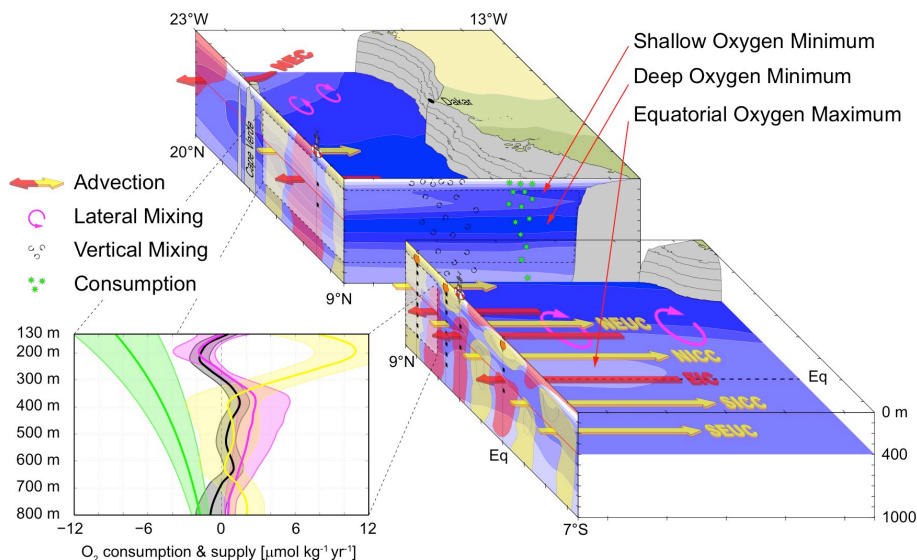


Figure 21. Schematic of the functioning of the ETNA OMZ and its oxygen budget. In the upper box, the oxygen distribution (bluish colours with dark/light blue corresponding to low/high oxygen) is shown at the sections along 23° W and 9° N and at the depth of 400 m; in the lower right box it is shown at the section along 23° W and at the depth of 400 m. Red and yellow areas at the 23° W section correspond to westward and eastward flow also marked by red and yellow arrows, respectively. The oxygen budget (lower left panel) includes physical supply by meridional (violet curve) and vertical mixing (black curve) as well as consumption after Karstensen et al. (2008) (green curve). The yellow curve in the lower left panel is the residual of the other 3 terms, which is dominated by zonal advection. All error estimates (coloured shadings) are referred to a 95 % confidence [except the isopycnal meridional eddy supply, where the error was estimated from both the error of the oxygen curvature (95 % confidence) and the error of the eddy diffusivity (factor 2 assumed)] (see further details in text and in Hahn et al., 2014).

[Title Page](#)
[Abstract](#)
[Introduction](#)
[Conclusions](#)
[References](#)
[Tables](#)
[Figures](#)
[Back](#)
[Close](#)
[Full Screen / Esc](#)
[Printer-friendly Version](#)
[Interactive Discussion](#)